

Aus der Medizinischen Klinik und Poliklinik I
Klinikum der Ludwig-Maximilians-Universität München
Direktor: Prof. Dr. med. Steffen Massberg

Regulation of Macrophage Regnase-3 in Cardiovascular Disease

Dissertation
zum Erwerb des Doktorgrades der Medizin
an der Medizinischen Fakultät der
Ludwig-Maximilians-Universität zu München

vorgelegt von
Jiahui Fang
aus
Qiqihaer, China
2021

Mit Genehmigung der Medizinischen Fakultät
der Universität München

Erster Gutachter: Prof. Dr. med. Christian Schulz
Zweiter Gutachter: Prof. Dr. med. Markus Sperandio
Dritter Gutachter: Prof. Dr. Alexander Bartelt
Dekan: Prof. Dr. med. dent. Reinhard Hickel
Tag der mündlichen Prüfung:11.03.2021.....

Affidavit



Affidavit

Fang, Jiahui

Surname, first name

Street

Zip code, town, country

I hereby declare, that the submitted thesis entitled:

Regulation of Macrophage Regnase-3 in Cardiovascular Disease.

is my own work. I have only used the sources indicated and have not made unauthorised use of services of a third party. Where the work of others has been quoted or reproduced, the source is always given.

I further declare that the submitted thesis or parts thereof have not been presented as part of an examination degree to any other university.

Qiqihaer, 28.03.2021

Fang, Jiahui

Place,date

Signature doctoral candidate

Contents

I.	Introduction	1
1.	Immune System	1
2.	Macrophage	2
2.1.	Macrophage Origin	3
2.2.	Macrophage in Heart.....	5
2.3.	Macrophages in Inflammation.....	5
2.4.	Macrophages in Fibrosis.....	7
3.	Regnase	7
3.1.	Regnase Family Member	7
3.2.	Regnase-3	8
4.	Cardiovascular Diseases and Myocardial Remodeling	9
4.1.	Hypertensive Heart Disease.....	10
4.2.	Myocardial Infarction	13
II	Aim of this Project.....	19
III.	Material and Methods.....	20
1.	Mice	20
2.	Mouse Experiments.....	20
2.1.	Anesthesia.....	20
2.2.	Induction of Cardiac Fibrosis.....	22
2.3.	Cardiac Ischemia Reperfusion Injury.....	23
2.4.	Tail vein injection of Mfge-8-GFP	26
3.	Flow Cytometry.....	28
3.1.	Sample Preparation for Flow Cytometry	28
4.	Histological examination	30
4.1.	Immunofluorescence staining.....	30
4.2.	Masson Goldner Trichome Staining.....	32
4.3.	Sirius Red / Fast Green staining.....	33
4.4.	TUNEL assay.....	34
4.5.	Histological Evaluation	34
5.	qPCR of mRNA levels	35
6.	Statistical Analysis	36
IV.	Results	37
1.	Regnase-3-deficient Mice at Steady State.....	37
1.1.	Cardiac Fibrosis at Steady State	37
1.2.	Cardiac Macrophage Number at Steady State	39
1.3.	Cardiac Inflammatory Factors at Steady State	40
2.	ANG II Mouse Models	43
2.1.	LysM-Cre; Regnase-3 ^{fl/fl} mouse strain.....	43
2.2.	Rank-Cre; Regnase-3 ^{fl/fl} mouse strain	46
3.	Ischemia Reperfusion Injury Mouse Models.....	52
3.1.	Mfge-8 efficacy to Detect Apoptosis	52
3.2.	LysM-Cre; Regnase-3 ^{fl/fl} mouse strain.....	54

3.3. Rank-Cre; Regnase-3 ^{fl/fl} mouse strain	54
V. Discussion.....	59
1. Mouse Model Methodology	59
2. Efficiency of Depleting Macrophage Regnase-3	60
3. The Identification of Fibrosis	60
4. Regnase-3 Deficient Mice at Steady State	61
5. Macrophage-specific Regnase-3 deficient mice of ANG II Infusion Models	63
6. Macrophage-specific Regnase-3 deficient After Ischemia/ Repertfusion.....	65
7. Outlook.....	65
VI. Summary	67
VI. Zusammenfassung	68
VII. Abbreviations.....	70
VIII. Acknowledgement.....	73
IX. References.....	75

I. Introduction

1. Immune System

The immune system is fundamental for human survival, and it is divided into two kinds of responses, adaptive and innate^{1,2}. Adaptive immune responses are also called acquired responses, including natural killer (NK) cells, B cells, and T cells. The immune cells of the adaptive immune response are activated by exposure to infections. Antigen-specific receptors are expressed on the surface of B and T lymphocytes, to form complete immunoglobulin gene products and T-cell receptors (TCR)³. Innate immune responses are also called natural responses which include basophils, mast cells, eosinophils, neutrophils, dendritic cells, monocytes, and macrophages. It is the first barrier to defense against infections and develops itself to regulate adaptive responses⁴.

As a matter of fact, innate and adaptive immunity are not existing independently; they communicate all the time and act together even though they have entirely different mechanisms. When the invading microbes try to attack the host for the first time, the innate immune cells start to approach and digest them, which process is called phagocytosis, then if the infection could not be cleared up, the lymphocytes will be activated and start to amplify such like antigen-specific B and T cells. These cells have the ability of memory and adaptation; they undergo clonal expansion and react faster and more effectively when the infection tries to attack the host the next time^{2,3}.

Innate immune cells have the ability to identify pathogen-associated molecular patterns (PAMPs), which are small motifs, and they can be triggered by Toll-like receptors, such like TLR4. Janeway and colleagues found that a continuously active mutant of TLR4 could activate nuclear factor κ B (NF- κ B)-controlled

genes such like interleukin -1(IL-1), IL-6, and IL-8⁵. TLR4 signaling can activate especially neutrophils and macrophages recruitment, which saves time for the following adaptive responses. Majority of the TLRs are single-pass transmembrane proteins on the surface of the cells, and they could be discovered on dendritic cells and macrophages. Their activation connects with acute or chronic inflammation⁶. However, disorders of innate responses will result in autoinflammatory diseases⁷.

Antibodies one hand bind to the antigens, which is well known; on the other hand, they signal to lymphocytes. At first, scientists wondered how the antibodies were made, and then they discovered that antigen-presenting cell (APC) and a leucocyte which can recognize the antigens on the APCs, were quite essential. These antigen receptors on lymphocytes are known as major histocompatibility complex (MHC), and they named human leukocyte antigens (HLAs) as well. There are two types of MHC, class I and class II MHC molecules, APCs present antigens to both of them. However, class I present peptide fragment synthesized in APCs, class II present extracellular compartment. T cells will then be activated through TCRs, either kill the cells presenting antigens or assist producing antibodies^{3,7}.

2. Macrophage

Macrophages were first discovered by the father of innate and cellular immunity Metchnikoff at the end of the 19th century. He made tremendous progress on phagocytic cells⁸. Later in 1969, a group of scientists dealt with the new concept of the mononuclear phagocytosis system (MPS). All cells with similar properties, morphology, kinetics, origins, and abilities, were assigned to this system, including progenitor cells and promonocytes in the bone marrow, as well as monocytes and macrophages in the tissues⁹. After discovering that peritoneal macrophages were unable to multiply by labeling studies with ³H-thymidine at

steady state, they began to investigate the origin of the macrophages using X-irradiation experiments on mice. Scientists finally realized that peritoneal macrophages were derived from blood monocytes, which in turn were produced in bone marrow¹⁰.

2.1. Macrophage Origin

It was believed for many decades that monocytes were the only source of macrophages, however recently, there has been increasing evidence showing that the yolk sac serves as a second source of macrophages. Various studies have shown that, under steady-state conditions, so-called steady-state tissue macrophages are derived from progenitor cells that colonized the embryo from the yolk sac before the development of definitive hematopoiesis began¹¹⁻¹³.

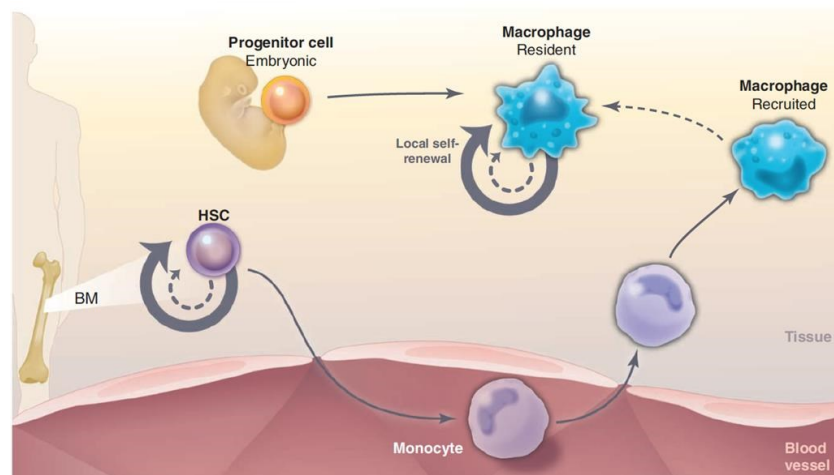


Figure 1 Macrophage self-renewal and differentiation. From Sieweke, et al. Beyond Stem cells: Self-renewal of Differentiated Macrophages. *Science*. 2013¹⁴. Copyright © 2013

In mice, macrophages can be detected in the yolk sac from day 8 of embryological development (E8). Definitive hematopoietic stem cells only appear in the aortic-gonadal mesonephros (AGM) region on day 10.5 and migrate from there to the fetal liver. They multiply and differentiate in the fetal liver from day 12.5^{11,15}. In humans, the hematopoiesis of the yolk sac begins around the third week of pregnancy and lasts three to six weeks. Definitive

hematopoiesis begins in the fifth to seventh week of pregnancy in the AGM region of the embryo. From the fourth and fifth to the 22nd week of pregnancy, hematopoiesis occurs in the liver in the meantime¹⁶.

It is also found that macrophages have the ability to self-renewal independently of hematopoietic stem cells (HSCs). As matured cells, macrophages are able to re-enter the cell cycle when they come across specific stimulations or injury. The ability for proliferation and self-renewal does not exclude an original lineage of HSCs¹⁴. Of course, despite HSCs and macrophages, T cells and polyploid hepatocytes also have the capacity to self-renewing^{17,18}.

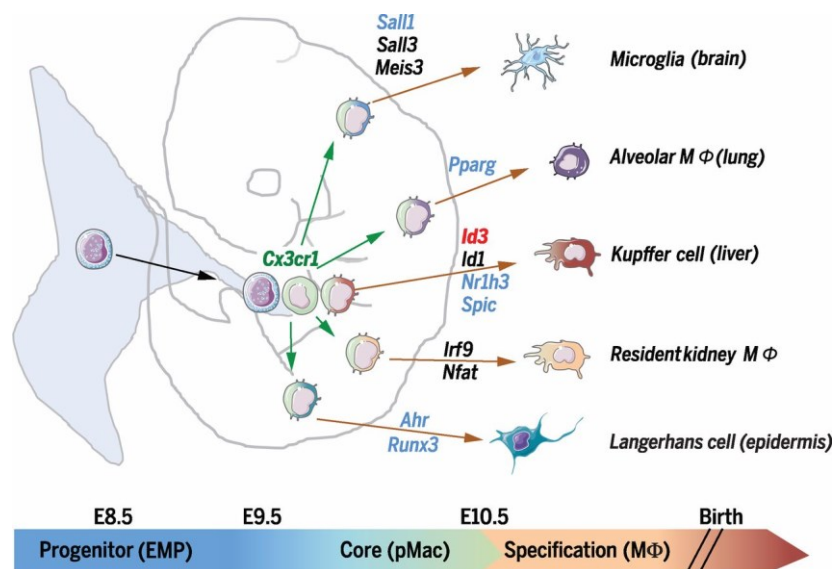


Figure 2 Tissue-resident macrophage development in mice. From Elvira Mass, et al. Specification of tissue-resident macrophages during organogenesis. *Science*. 2016¹⁹. Copyright © 2016

Many indications show that the compositions of the macrophages change in the course of life and together with their properties and functions. For example, in newborn mice, cardiac macrophages show an MHC-II⁻ phenotype and originate primarily from the yolk sac. These macrophages appear to have a positive effect on the myocardium under stress conditions. However, with age, MHC-II⁻ macrophages gradually develop into MHC-II⁺ after six weeks. The

surface molecule chemokine (C-C motif) receptor 2 (CCR2) is the receptor of the chemokine ligand 2 (CCL2) also called as monocyte chemoattractant protein-1 (MCP-1), and it enables monocytes to undergo chemotaxis and thus migrate from the bone marrow into the bloodstream. This surface molecule can be used to identify macrophages that have recently been derived from circulating monocytes. CCR2 and MHC-II can define subgroups of cardiac monocytes and macrophages in newborn and adult mice^{20,21}.

2.2. Macrophage in Heart

Macrophages can be found in all tissues of the body. They are a critical part of the immune response and contribute to homeostasis and tissue repair by phagocytizing pathogens and secreting cytokines and chemokines. In addition to general tasks, they also perform organ-specific tasks depending on the location²².

The heart is also included. Cardiac macrophages are widely accepted to play an important role both under steady state and in cardiac injury. Recently, it has been reported that macrophages populate the healthy and injured myocardium, given that several subtypes can be found and classified in heart^{23,24}. Two subsets of cardiac macrophages are found by the in-depth phenotyping under steady state, MHC-II^{lo}CCR2⁻ and MHC-II^{hi}CCR2⁻ cells. Besides, MHC-II^{hi}CCR2⁺ cells can be detected under cardiac inflammation²⁰.

2.3. Macrophages in Inflammation

10% to 15% in most tissues are macrophages; they are required to clear the apoptotic cells under steady state and respond to inflammation when there is infection or injury. In mice, inflammatory monocyte (lymphocyte antigen 6 complex, Ly6C^{hi}) are differentiate into macrophages when they are recruited from circulation to the affected or injured tissue. These macrophages, at early

stage, show a pro-inflammatory phenotype, however, they switch into an anti-inflammatory phenotype in order to control the disease progression. M1 type macrophages, which is named classically activated macrophages as well, can be induced by infections and release cytokines. However, alternatively activated macrophages, M2 macrophages, are induced by Th2 cytokines. According to different states, M1 and M2 types can alter into one another. Basically, four schematic steps happen during inflammation: pathogen recognition, immune cells recruitment, elimination and resolution. Danger associated molecular patterns (DAMPs), including high mobility group box-1 (HMGB1), RNA, DNA, S100 proteins and histones, are recognized by the pattern recognition receptors (PRRs) expressed by innate cells. Innate immune system is first triggered by TLRs and nucleotide-binding oligomerization-domain protein like receptors (NLRs), then result in releasing many chemokines and cytokines which including tumor necrosis factor- α (TNF- α), IL1 and IL-6. Tissue resident and recruited macrophages eliminate the infectious agents afterward and enable the resolution of inflammation in order to keep the tissue back to homeostasis. However, in order to maintain the organ function, tissue repair and fibrosis are initiated by type-2 which is related to IL-4, IL-5, IL-9, IL-13, IL-25, IL-33, IL-4- and IL-13-activated macrophages²⁵⁻²⁷.

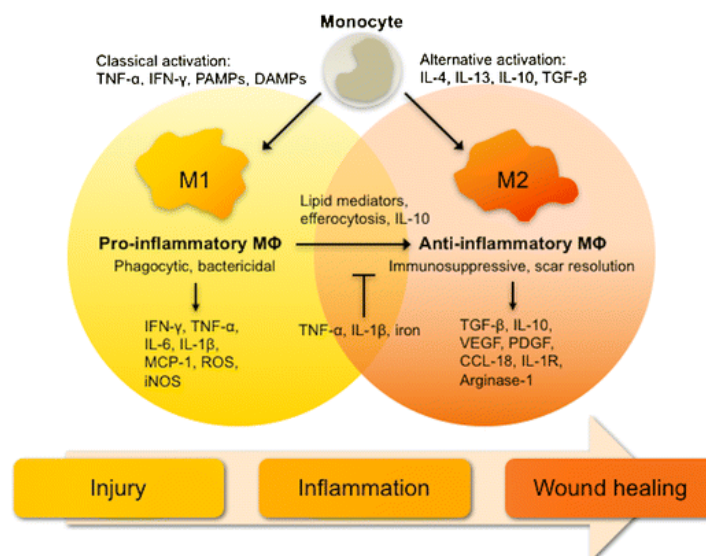


Figure 3 Evolution of macrophage function under repair. From Kate S. Smigiel and William C. Parks. Macrophages, Wound Healing, and Fibrosis: Recent Insights. *Current Rheumatology Reports*. 2018²⁸. Copyright © 2018

2.4. Macrophages in Fibrosis

Macrophages and their products are involved in every step of tissue and wound healing. Previous studies showed that M2 macrophages are the primary type or subsets in promoting scar and fibrosis formation. However, recently this concept has been challenged, several studies have described that M2 type macrophages are working to reduce the fibrosis and inflammation, but not the opposite²⁸. But this phenomenon only happens in the liver, there is still more needs to be studied among other organs and models. Type 2 macrophages are reported to regulate tissue repair and pathological fibrosis in many organs, among these, IL-13- and IL-4-activated macrophages have an important role. Macrophage-secreted matrix metalloproteinase 12 (MMP12) produced by this type of macrophages, can control other types of MMPs, in this way, matrix degradation reduces and fibrosis formation increases. IL-4- and IL-13-activated macrophages can also regulate fibroblasts by several factors, including growth factor family members, transforming growth factor- β (TGF- β) and platelet-derived growth factor (PDGF),²⁹.

3. Regnase

3.1. Regnase Family Member

During pro- and anti-inflammatory pathways, RNA-regulating factors and post-transcriptional networks play a critical role, among these, the Regnase family members which were found in the last decade have shown activities in immune cells. The Regnase family was first named as monocyte chemotactic protein-induced proteins (MCP1P1-4), encoded by Zc3h12a, Zc3h12b, Zc3h12c and

Zc3h12d³⁰. However, during later studies, scientists found that MCPIP1 had the ability to work as an RNase, so they renamed the MCPIP1 as regulatory RNase-1 (Regnase-1), widely used by now³¹. The most investigated Regnase family member is Regnase-1, it is reported to be regulated by NF-κB pathways, and after deletion of Zc3h12a gene in mice, macrophages show higher expression of IL-6 and IL-12p40 in reaction to TLR ligands³². Regnase-1 was also described to control the post-transcriptional regulation of inflammation together with Roquin³³.

RNA-binding proteins are rapidly emerging during recent years acting as effectors and regulators in cardiovascular diseases³⁴. They involve in each process of the post-transcriptional regulatory mechanisms, including pre-mRNA alternative splicing, mRNA editing, transcript stability and localization³⁵. RNA-binding proteins are reported to participate in the development of the heart as well, from the cardiac establishment to maturation³⁵. By regulating the transcriptome through phenotype switching, RNA-based potential therapeutic treatments may provide new insights into clinical trials.

3.2. Regnase-3

Recently, Matthias von Gamm and his colleagues reported that Regnase-3 is required in immune homeostasis and specifically regulated by interferon regulatory factor (IRF) signaling. In that study, they used *Regnase-3*-deficient mice to investigate their physiological character. Because of the miss of Regnase-3 in macrophages, severely lymphadenopathy was found in *Regnase-3*^{-/-} mice, however there was no systemic autoimmunity. In contrast with Regnase-1, Regnase-3 depends on interferon (IFN) pathway. In *Regnase-3*^{-/-} mice, IFN-γ, MHC-II and Stat1 are together up-regulated. They also demonstrated that Regnase-3 could be related to degrading extracellular material because of its localization and little change in gene expression. Like

Regnase-1, Regnase-3 can also bind mRNA at 3' untranslated regions (UTRs) and degrade RNA³⁶. The function of Regnase-3 in macrophages remains to be investigated in disease models. In this study, we apply inflammatory cardiac mouse models on Regnase-3 specific deletion both in myeloid lineage and tissue-resident macrophages in order to find out the potential therapeutic targets in cardiovascular diseases.

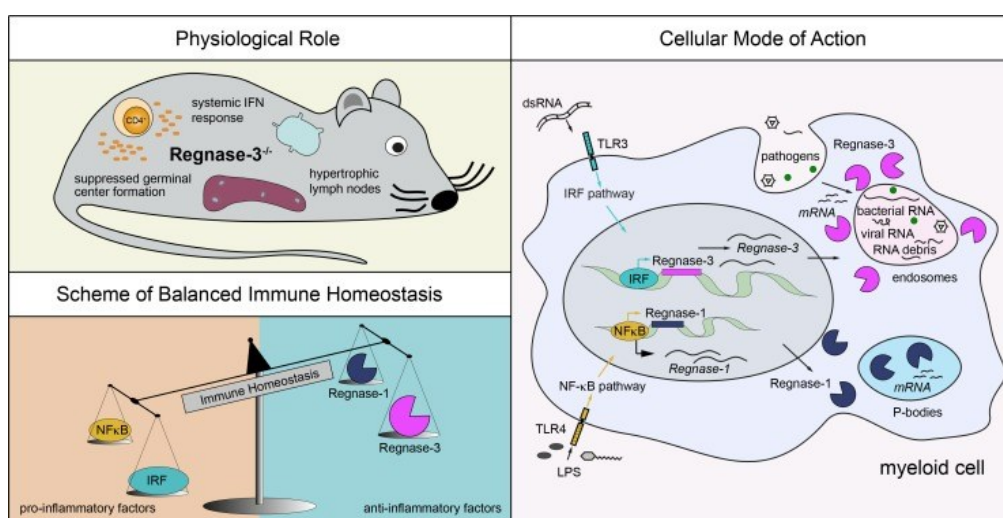


Figure 4 Difference between Regnase-1 and Regnase-3. From Matthias von Gamm, et al. Immune homeostasis and regulation of the interferon pathway require myeloid-derived Regnase-3. *J Exp Med.* 2019³⁶. Copyright © 2019 von Gamm et al.

4. Cardiovascular Diseases and Myocardial Remodeling

In both developed and developing countries, the cardiovascular disease presents high morbidity and mortality, especially myocardial infarction and chronic ischemic heart disease³⁷.

4.1. Hypertensive Heart Disease

4.1.1. Angiotensin II in Hypertensive Heart Disease

It has been reported that hypertension is a major health factor in cardiovascular disease, which induces left ventricular hypertrophy, both diastolic and systolic dysfunction, arrhythmias and even heart failure³⁸. During this process, angiotensin II (ANG II) is considered as a well-established mediator to promote cardiac remodeling via increasing inflammatory responses and stimulating several profibrotic factors through numerous signaling pathways^{39,40}. It is a peptide hormone which is produced from ANG II by the circulating angiotensin converting enzyme (ACE) formed both in endothelial cells and the vasculars⁴¹. The renin-angiotensin-aldosterone system (RAAS) has a critical effect in human body fluid and blood pressure which will directly or indirectly leads to cardiac remodeling and cardiovascular disease. As the main effector peptide, ANG II binds both type-1 receptor (AT₁R) and type-2 receptor (AT₂R), whereas they have opposite functions. Accumulating evidence also has shown that these two receptors not only regulated by ANG II, but also by their associated proteins^{41,42}. During activation of RAAS, inflammation and fibrosis formation developed⁴³.

4.1.2. Inflammation in ANG II-induced Hypertrophy

ANG II, inflammation and immune response are related to one another. In the cardiovascular system, ANG II has a vital part in the physiological and pathological process which associated with inflammation and proliferation. It can increase the expression of pro-inflammatory markers such like IL-1 β , IL-6, MCP-1, vascular cell adhesion molecule-1 (VCAM-1) and pro-inflammatory transcription factor NF- κ B^{44,45}. Long term inflammation process activates reactive oxygen species (ROS) which on the contrary causes endothelial

dysfunction and oxidative stress⁴⁶. ANG II is also involved in inflammatory processes by recruiting leukocytes via the expression of the vascular endothelial growth factor (VEGF) and increasing the vascular permeability, adhesion molecules and chemokines such as MCP-1^{40,47,48}. Besides, ANG II triggers the release of monocytes from the spleen, which, unlike bone marrow-derived monocytes, takes place independently of chemokine receptor 2⁴⁹. It also has been reported that ANG II involves nearly all kinds of cardiovascular disease, it can induce the Ly6C⁺ monocytes influx and differentiated into CD11c^{lo} MHC-II^{lo} and Ly6C⁺ macrophages. Mice receiving ANG II result in increased TLR4, and this suggests that the peripheral activation is before the infiltration²⁰.

4.1.3. Fibrosis in ANG II-induced Hypertrophy

Fibrosis is fundamental in hypertensive heart disease due to myocardial structural remodeling. It is defined hardening and scarring of the heart tissues because of the continuous infections, immune responses, radiation and tissue injury. The fibrous tissue formation, which myofibroblasts are involved in, is modulated at the sites of locally generated ANG II and endothelin-1^{50,51}. Whereas the myofibroblasts can differentiate from fibroblasts which can express lots of pattern recognition receptors including Toll-like receptors, thus, Toll ligands, in turn, activate fibroblasts transforming into myofibroblasts. Persistent inflammatory reactions, tissue necrosis and infections can lead to chronic activation of fibroblasts and myofibroblasts and thus to a continuous deposition of components of the extracellular matrix, such as hyaluronic acid, fibronectin, proteoglycans and collagen. As a result, a permanent fibrotic scar often arises⁵². Inflammatory processes and fibrotic changes play a critical role in the progression and development of cardiovascular diseases^{53,54}. ANG II involves in the fibrosis process as well by producing TGF- β , PDGF and reduces the activity of the interstitial metalloproteinases^{55,56}. However, most of the

effects are mediated by AT₁R but not AT₂R. Crowley et al. showed that the AT₁R in the kidney is particularly responsible for the development of ANG II-dependent hypertension and cardiac hypertrophy⁵⁷. Calpain activation was also reported to involve in the ANG II-induced cardiac remodeling via the NF-κB pathway⁴⁰.

4.1.4. Role of Macrophages in ANG II induced Hypertrophy

Since macrophages participate in each step of inflammation and fibrosis formation, ANG II-induced cardiac hypertrophy involves many cytokines and chemokines related to macrophages. ANG II can stimulate IL-6 production and result in macrophage recruitment and MCP-1 expression. Factors like ANG II involved in hypertension will also stimulate enzyme sources for example, nitric oxide (NO) synthase and nicotinamide adenine dinucleotide phosphate (NADPH) oxidase, which will in turn promote hypertension. Macrophages are the main source to kill pathogens by producing ROS, which is also the production of NADPH oxidase in the vasculature. By releasing ROS, macrophages can exacerbate ongoing oxidation. Hypertension prevention is also reported to relate with the decreased IL-6 expression, macrophages and T cell infiltration⁴⁶. Bush and colleagues also found that in mice, ANG II-induced hypertension, CCR2 is required for macrophages infiltration and vascular hypertrophy⁵⁸. MMP-12, a macrophage-secreted elastase, was also demonstrated to involve ANG II-induced heart fibrosis and M2 macrophage accumulation⁵⁹. Slava Epelman and colleagues found that ANG II caused the increased expression of MHC-II^{hi} CD11c^{hi} macrophages and decreased the expression of MHC-II^{hi} CD11c^{lo} macrophages, which indicates that under pressure condition, macrophage subsets have different functions. They also found that after ANG II infusion, CCR2⁻ MHC-II^{lo} macrophages subpopulation had the maximal expression in heart²⁰.

4.2. Myocardial Infarction

Acute myocardial infarction triggers inflammatory activation and remodeling processes in the heart. This leads, among other things, to the loss of functional tissue and, through wound healing, to the development of fibrosis, which leads to stiffening of the heart muscle⁶⁰.

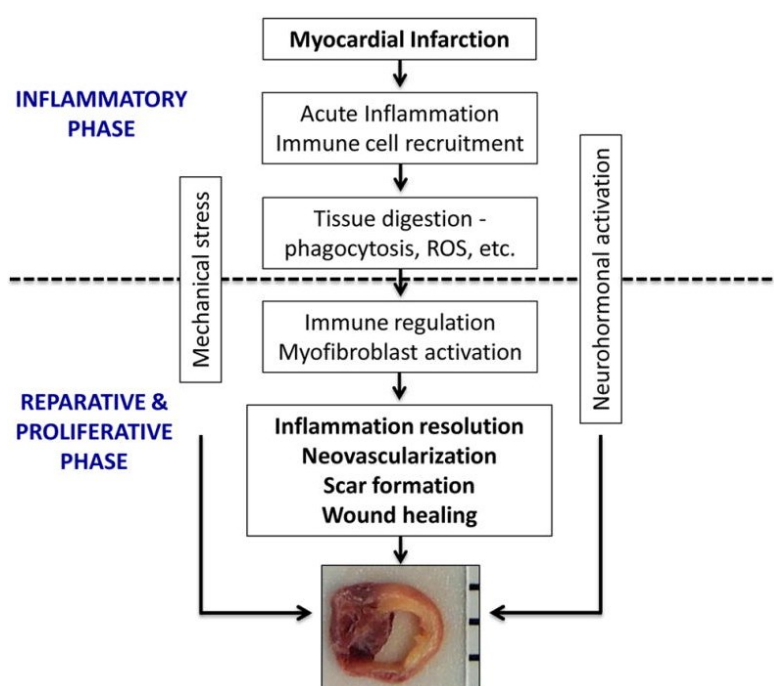


Figure 5 Steps of cardiac repair after myocardial infarction in mice. Sumanth D. Prabhu and

Nikolaos G. Frangogiannis. *Circ Res.* 2017⁶⁰. Copyright © 2016, Wolters Kluwer Health

4.2.1. Inflammation during Myocardial Infarction

Both molecular and cellular signaling are involved in the inflammatory process after severe myocardial ischemia^{61,62}. Hypoxia, the lack of oxygen supply, destroys the vessels' integrity and barrier, and results in a set of sterile inflammation, cardiac myocytes necrosis and leukocyte infiltration^{63,64}. DAMPs, which can trigger the inflammatory response, are secreted and released during this process, they bind to the PRRs such as TLRs, NLRs and Receptor of Advanced Glycation End-Products (RAGE), these on the contrary leads to the

activation of immune cell and the release of pro-cytokines⁶⁵. Single-stranded ribonucleic acid (ssRNA), HMGB1, S100A, IL-1 α , double-stranded ribonucleic acid (dsRNA) and all resemble DAMPs. In humans, HMGB1 can serve as a predictor of left ventricular dysfunction since it will increase after AMI⁶⁶. Through TLR2, TLR4 and TLR9, NF- κ B signaling can be activated by HMGB1, whereas TLR3 can be stimulated by dsRNA⁶⁷. TLRs are the main PRRs in human cells, except TLR3 and TLR7-10, most of them are cell-surface receptors, they express in the intracellular compartments⁶⁸. TLRs signaling is reported to involve MI, deficiency of TLR2 or 3 or 4 shows reduced infarct size in mouse models after I/R⁶⁹⁻⁷¹.

Pro-inflammatory cytokines are upregulated after MI due to the downstream signaling of MAPK and NF- κ B pathway or by the expression of infiltrating cells or leukocytes recruitment. IL-1, IL-6, IL18, TNF are the primary mediators in the injured myocardium, however in mouse models, not all the deficiency mediators act to attenuate ischemic heart or remodeling. For example, TNF^{-/-} mice show smaller infarct size⁷², whereas IL-6 deficiency mice show no change in size or remodeling⁷³. These data demonstrate that the effects of the cytokines and chemokines are complex in vivo microenvironment and they cannot be simply regarded as good or bad⁶⁰.

Two waves of monocytes recruitment can be observed, the early stage lasts 3-4 days after the infarction, whereas the late stage at around 7 days after the infarction occurs. Inflammatory Ly6C^{high} CCR2⁺ CX3CR1^{low} monocytes (78%) are found in the early phase in response to MCP-1/CCL2 expression, whereas in the late phase non-inflammatory Ly6C^{low} CCR2⁻ CX3CR1^{high} monocytes make up the largest share with approximately 80%. The phagocytic activity was approximately the same in both subgroups, but Ly6C^{high} monocytes also showed a high proteinase activity in the extracellular matrix, which played a critical part in the process of degradation. Ly6C^{high} monocytes also produce the

proinflammatory IL-1b, cytokine tumor necrosis factor- α (TNF- α), MMPs and cathepsins. In contrast, the non-classical Ly6C^{low} monocytes express VEGF, TGF- β and IL-10. The inflammatory Ly6C^{high} monocytes consequently have proteolytic and inflammatory functions, whereas Ly6C^{low} monocytes have proangiogenic and reparative properties. The sequential recruitment and the different functional properties indicate different tasks in the healing process of the heart. It is the task of the Ly6C^{high} monocytes to break down the dead tissue so that Ly6C^{low} monocytes can then support the healing process through angiogenesis, accumulation of myofibroblasts and accumulation of collagen for a stable scar^{60,74,75}.

In the first week after myocardial infarction, significantly more monocytes than macrophages are detectable in the myocardium. From the second week on, macrophages and dendritic cells predominate again independence from blood monocytes⁷⁶. The immigrated monocytes came from both the bone marrow and the spleen. Since monocytes have an average lifespan of around 20 hours, the population must be able to be replaced within this time. To enable this high turnover of monocytes, the spleen in mice and humans release the monocytes stored there and start extramedullary monocytopoiesis, which is triggered by IL-1. Although they were the first leukocyte population to reach a stable peak at 24 hours after the infarction, they subsequently decreased steadily⁷⁷.

Two different subtypes of monocytes could be described in humans as well. Mouse resident monocytes are alike to human CD14^{low} CD16⁺ monocytes, mouse inflammatory monocytes are alike to human CD16⁺ CD14⁺ monocytes. Even though the subgroup-specific gene expression in humans and mice has been partially preserved, some differences in gene expression should be taken into account when transferring results^{74,78}.

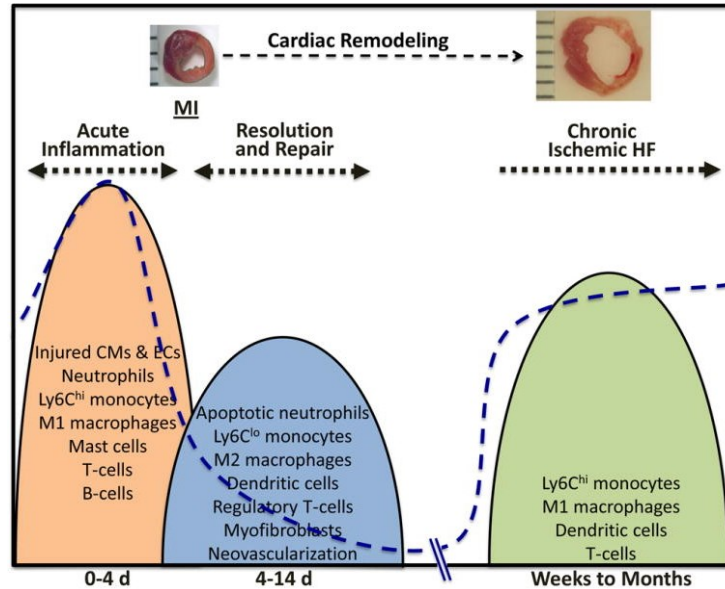


Figure 6 Inflammation after myocardial infarction in mice. Sumanth D. Prabhu and Nikolaos G.

Frangogiannis. *Circ Res.* 2017⁶⁰. Copyright © 2016, Wolters Kluwer Health

4.2.2. Macrophage in early Myocardial Infarction

In mice heart, around 5% to 10% of nonmyocytes are tissue resident macrophages at steady state with diverse phenotypes^{76,79}. As the largest cardiac resident populations, macrophages are also abundant after MI and most of them derive from circulating monocytes both at infarct tissue and remote myocardium. It was reported that on day 5 the infarct area showed peak numbers of recruited cells and day 10 for the remote area⁸⁰. Once recruited, the differentiated macrophages expressed F4/80 will stay at a high level for few days after ischemia. Their main functions are removing debris of dead cells, expressing inflammatory cytokines and involving in cardiac remodeling⁷⁹. In mice with LAD (left anterior descending artery) ligation, macrophages numbers still remain high even months later⁸¹.

It is also reported that, in adult heart, after inhibiting the monocyte recruitment, embryonic-derived macrophages were preserved after MI which leading to a decreased inflammation and increased coronary angiogenesis. Furthermore,

the neonatal macrophages are critical for the recovery of injured heart⁸². However, we still have to keep in mind that in neonatal mice following MI before postnatal day 7, the heart can fully recover without scar formation, after that, the heart loses the ability of regeneration and angiogenesis, then turned into fibrosis and scar formation in adult⁸³.

Cardiac macrophages are divided into several subsets according to MHC-II and CCR2 expression, yolk sac derived MHC-II^{lo}CCR2⁻ and MHC-II^{hi}CCR2⁻ macrophages, and monocytes derived MHC-II^{hi}CCR2⁺ macrophages. Resident macrophages are gradually replaced by bone marrow and spleen derived monocytes over time⁸⁴. During the inflammatory stage of MI, as early as 30 minutes, Ly6C^{hi} monocytes are recruited into infarct area in first 4 days through MCP-1/CCR2 interactions and differentiate into macrophages to digest dead cells and debris⁸⁵. Ly6C^{lo} monocytes are recruited from day 5 via the CX3CR1 pathway and transform into macrophages. Moreover, the Ly6C^{hi} cells can also differentiate into Ly6C^{lo} cells locally in the healing stages⁸⁶.

M1 and M2 macrophage phenotypes are classified by their functions. M1 macrophages are predominantly found in the first three days after infarction, however later by one week, M2 macrophages are found major⁸⁷. It is also demonstrated that M1 macrophages exist too long will lead to enlarged infarct size and prevent the process of inflammation and cardiac remodeling. On the contrary, M2 macrophages show the capacity to improve cardiac healing and resolution of the inflammatory process and fibrosis post MI⁸⁸. It is inferred that M1-like macrophages are derived from circulating Ly6C^{hi} monocytes, whereas M2-like macrophages are from Ly6C^{lo} monocytes. In vitro, M1 macrophages can be activated by IFN- γ , LPS and GM-CSF, whereas IL-4, IL10 or TGF- β can achieve M2 macrophages. However, heart microenvironment must take into account when it comes to vivo polarization^{76,88}. When M1 phenotype polarizes into M2 macrophages, it marks the start of proliferative phase post MI⁸⁹.

4.2.3. Cardiac Remodeling after Myocardial Infarction

The inflammation phase is followed by a proliferation phase in which a new matrix is formed to stabilize the left ventricle. If the course of this phase was impaired, the ventricle would become dilated or even ruptured. The non-inflammatory phase will end with the formation of an acellular, collagenous scar⁷⁹. Cardiac remodeling can be divided into an early and a late phase. While the early phase takes place in the first three days after the infarction and affects the infarct and peri-infarct zone, the late phase takes place from the third day and involves the entire left ventricle in the remodeling processes⁶⁰.

During cardiac remodeling, fibrosis formation has resembled as a hallmark and it appears to be an irreversible process. After MI, replacement fibrosis becomes dominant and essential to replace dead tissues and start repair program⁹⁰. In order to protect the heart from rupture and preserve the integrity of the heart ventricle, a fibrous scar becomes a predictor of adverse outcome⁹¹.

Due to the high prevalence of heart diseases, this project deals with these two different inflammation mouse models to better understand the process of cardiac remodeling, fibrosis formation and the relationship with macrophage Regnase-3. In a chronic inflammation model, treatment with ANG II can trigger the development of cardiac fibrosis. Acute myocardial infarction is induced in mice by transient ligation of the LAD.

II Aim of this Project

Although Regnase-3 has been reported act specifically within myeloid cells, little is known about role of Regnase-3 during cardiac chronic inflammation and ischemia reperfusion injury. In this work, we used several Regnase-3 deficiency mouse strains to investigate their steady state roles, cardiac fibrosis formation and chronic inflammation. The goal is to contribute to developing new therapeutic strategies through a better understanding of the formation and regulation of inflammatory and fibrotic processes in the heart.

III. Material and Methods

1. Mice

C57BL/6J, LysM-Cre mice were purchased from The Jackson Laboratory. Rank-Cre mice were obtained from Yasuhiro Kobayashi (Nagano, Japan)⁹². Mice with the knockout-first allele for Regnase-3, Regnase-3^{fl/fl} and ROSA26-Cre;Regnase-3^{fl/fl} mice were designed and generated by EUCOMM database³⁶. Regnase-3^{fl/fl} mice were cross-bred to the LysM-Cre mice (B6.129P2-Lyz2^{tm1(cre)lfo/J}) to generate Regnase-3 ablation in myeloid lineage (LysM-Cre; Regnase-3^{fl/fl}). To generate Rank-Cre; Regnase-3^{fl/fl} mice, Regnase-3^{fl/fl} were cross-bred with Rank-Cre mice, in order to obtain Regnase-3 ablation in tissue-resident macrophages.

Older than 8 weeks age of mice, both male and female, were used for the experiments. All these animals were bred and kept in the animal facility of Walter-Brendel Zentrum and Neuropathologie und Prionforschung (ZNP) in Munich, Germany. Mice are maintained with sufficient food and water in stable temperature and air humidity. All the animal experimental protocols are based on German laws on animal protection and are approved by the German state government of Bavaria (licence numbers #55.2-1-54-2532-55-2015, 55.2-2532.Vet_02-16-183, ROB-55.2-2532.Vet_02-19-1, and ROB-55.2-2532.Vet_02-19-17).

2. Mouse Experiments

2.1. Anesthesia

Triple anesthesia from various injection anesthetics (medetomidine, midazolam and fentanyl, MMF) was used, the synergisms among which the dose to be

used could be reduced. In addition, the anesthetic regime used can be easily controlled and completely antagonized.

Medetomidine (Dorbene vet, Deutschland GmbH, Berlin) was used in a dosage of 0.5 mg/kg.

Midazolam (Midazolam, B. Braun, Melsungen) was used in a dosage of 5 mg/kg. It also provides a calming, anxiolytic and anticonvulsant effect.

The synthetically produced opioid fentanyl (Fentadone, Albrecht GmbH Aulendorf), the dosage used was 0.05 mg/kg. It is easy to control, but not suitable for postoperative analgesia. Therefore, the opiate buprenorphine (Buprenovet, Bayer Vital GmbH, Leverkusen) was used in the dose of 0.1 mg/kg to relieve postoperative pain.

In order to keep the stress load during the intraperitoneal injection of the combination anesthesia as low as possible, anesthesia was introduced with isoflurane (isoflurane CP, cp-pharma, Burgdorf). For this purpose, the mouse was placed in a transparent plexiglass tube which was connected one side to an evaporator (Datex-Ohmeda Isotec 5, UniVet Porta from Groppler, Deggendorf) and the other side to a suction device. A 5% isoflurane-oxygen mixture flowed into the tube via the evaporator. After a while, when the reflex was vanished, the mouse could be removed from the tube and the anesthetic administered intraperitoneally using a 30G cannula (BD Mikrolance, Becton Dickson GmbH, Franklin Lakes, USA) and a 1 ml syringe (Injekt-F, B. Braun, Melsungen). After the injection, the mouse was placed on a warm plate in an anesthetic box to protect it from light or other stimuli. To prevent the cornea from drying out, an eye ointment was applied (Bepanthen eye and nose ointment, Bayer, Leverkusen). The flexor reflex was checked before and at regular intervals during an operation and re-injected if necessary.

2.2. Induction of Cardiac Fibrosis

2.2.1. Preparation of an osmotic pump

To induce the development of cardiac fibrosis, mice were implanted with an ANG II-filled osmotic pump (a set of micro-osmotic pump, model 1002 for 14 days and model 1004 for 28 days, duresis Corporation, Cupertino, USA) under the skin. The mice received the active ingredient ANG II (ANG II human 10 mg, Sigma-Aldrich, St. Louis, USA) in a dosage of 1.8 µg/kg body weight /min. In order to achieve the stated dose, the active substance was diluted with NaCl accordingly. The filling volume was 100 µl, the pumping rate was 0.19 µl / h (model 1002) or 0.11 µl / h (model 1004). In this thesis, only model 1002 was used.

2.2.2. Pump Implantation

The mice were first anesthetized with combination anesthesia. In order to maintain the body temperature, the animals were placed on a warm plate (EHE-3503-CU-5WCR, FMI Föhr Medical Instruments, Seeheim / Ober-Beerbach) during the procedure. The eyes were covered with an ointment to protect them from drying out.

Next, the hair in the neck area was removed with a depilatory cream (depilatory cream asid-med, Asid Bonz, Herrenberg) and this area was then disinfected with iodine (Braunol, B.Braun AG, Melsungen). After reaching the surgical tolerance, which was checked using the inter-toe reflex, around 1 cm long skin incision was made in the depilated neck across the spine. With the help of scissors and tweezers, the subcutis was bluntly detached from the muscles on the right or left of the spine, creating a cavity that was large enough for the pump.

A pump filled with ANG II was placed into this cavity. The pump was aligned parallel to the spine and pushed as far caudal as possible to prevent movement restrictions in the neck area. The skin incision was then sewn with single button thread (7-0 Prolene). The animals received buprenorphine once to alleviate postoperative pain. The duration of the operation was around 10 minutes.

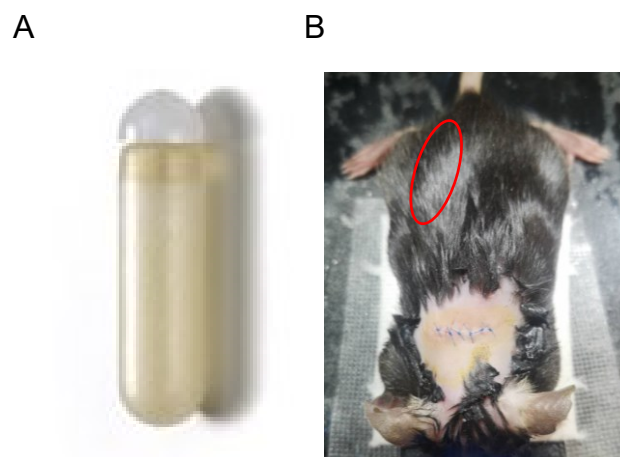


Figure 7 The micro-osmotic pump (A) and the mouse shown after pump implantation and skin incision was sewn (B). The red circle indicates the micro-osmotic pump's location under skin which put through the suture.

After the operation was completed, the anesthetic was antagonized. When the animal was awake enough, it was returned to its cage, which remained on the warm plate for the rest of the day. The general condition of the animals was regularly checked using a score sheet.

2.3. Cardiac Ischemia Reperfusion Injury

The ischemia reperfusion model was chosen instead of permanent ligation of the LAD because it is closer to the clinical situation. This makes the results more transferable to humans.

The mice were first anesthetized with the combination anesthesia described above. After the toe reflex was extinguished, they were fixed on the back with adhesive strips (Transpore, 3M Deutschland GmbH, Neuss) on a warm plate. The head came to rest on a cellulose swab (Orbis Dental, Münster) and the upper jaw was fixed with a commercially available rubber band, which was stretched around the heating plate, to facilitate intubation. The neck area and the left side of the chest were then depilated and disinfected with iodine.

After reaching the surgical tolerance, an approx. 1 cm long skin incision was made caudally along the trachea at the level of the larynx and the trachea was carefully dissected without damaging the mandibular gland. For intubation, the lower jaw was gripped with tweezers and the tube (19G metal cannula) was inserted into the pharynx. The tube was placed in the trachea under visual position control. The uniform raising and lowering of the chest served as a control of the correct intubation. Ventilation was performed using an intubation device (MiniVent Type845, Hugo Sachs Elektronik, March-Hugstetten) at a frequency of 150/min and a tidal volume of 200 μ l. The skin incision was sutured with single thread (7-0 Prolene, Ethicon, Johnson & Johnson Medical, Norderstedt).

Now the heating plate was carefully rotated 180 degrees and the mouse aligned under a microscope (Stemi 2000-C, Carl Zeiss, Jena) and a cold light lamp (CL 6000 LED, Carl Zeiss, Jena) so that the left side of the chest was in view. In order to maintain body temperature during anesthesia, a rectal probe (TMF-3402 rectal temperature sensor, FMI Föhr Medical Instruments GmbH, Seeheim / Ober-Beerbach) was introduced. This was connected to a temperature control module (-0904, FMI Föhr Medical Instruments GmbH, Seeheim / Ober-Beerbach), which in turn was connected to the warm plate. This self-regulating system kept the body temperature constant at 37.5 degrees. The next step was a skin incision at the level of the 2nd intercostal space. The

pectoralis muscle and rectus thoracis muscle were then severed so that the intercostal muscles were clearly visible. The 2nd intercostal space was opened with micro-scissors without injuring the mammary artery. In the next step, the 2nd and 3rd ribs were pierced twice with a thread (5-0 Prolene, Ethicon, Norderstedt) and stretched up or down by fixing the thread ends on the heating plate with adhesive strips.

In order to find the LAD better, the pericardium was opened and stretched over the lungs with a swab soaked in iodine (Sugi Eyespear pointed tip, Kettenbach, Eschenburg). The LAD is located at the lower edge of the left auricle and was pierced with an 8-0 thread (8-0 Prolene, Ethicon, Norderstedt). A placeholder was placed between the heart muscle and the double knot. A 30G cannula was threaded into a polyethylene tube for its manufacture. Then a 2-3 mm piece of it was cut off. In the next step, the double knot was tightened, and a second knot was placed on it. The success of the ligation of the LAD was checked on the fading of the myocardium. Now the holding threads were loosened and the open thorax was covered with a gauze compress soaked in 0.9% NaCl (Noba dressing agent Danz, Wetter) to protect the tissue from drying out.

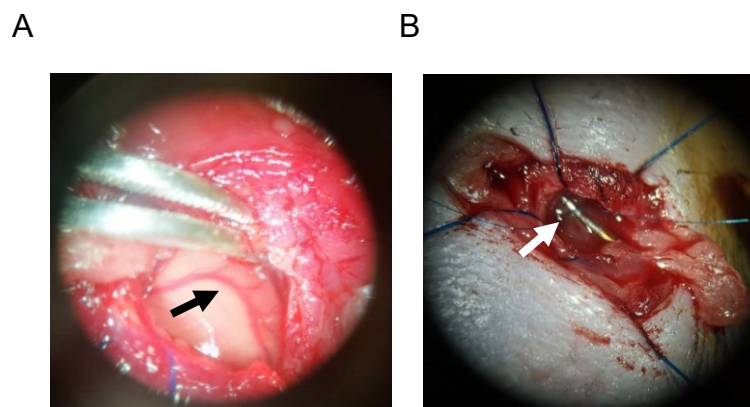


Figure 8 The indication of LAD ligation. The LAD shown on heart of mouse during surgery (A) and after ligation of LAD (B). The arrows indicate the LAD and ligature location.

Placeholders, knots and tethers were removed after 60 minutes. Then the intercostal muscles were first sutured with two to three single button thread (5-

0 Prolene, Ethicon, Norderstedt). The pectoralis muscle and the rectus thoracis muscle were also sutured with single button thread (7-0 Prolene, Ethicon, Johnson & Johnson Medical, Norderstedt). The skin suturing was continuous (7-0 Prolene) and the wound was then disinfected with iodine. The duration of the operation was approx. 90 minutes.

Then the anesthetic was antagonized. The animals were not extubated until they showed defense reactions and sufficient self-breathing could be assumed. When the mice were awake enough, they were placed in their cage and placed on a warm plate. For analgesia, the animals received buprenorphine for three days and were monitored using a score sheet.

2.4. Tail vein injection of Mfge-8-GFP

In order to inject total quantity of 50µg per mouse, mfge-8-GFP (0.98 mg/ml, from Thomas Brocker, BioMedizinisches Centrum der LMU, Germany) was diluted into 51µl with diluent buffer (from Thomas Brocker, BioMedizinisches Centrum der LMU, Germany). An appropriate intravenous catheter was made with a 5 cm long polyethylene tube (Portex, 0.28mm ID 0.61mm OD, Smiths Medical International, USA) and a cannula (30G, BD Microlance, Becton Dickinson Labware, USA) combined with a 1mL syringe (B. Braun, Germany). The diluted mfge-8 was pipetted into the syringe without air bubble, 0.9% NaCl was filled into the tube without air beforehand.

Mouse was anesthetized with a t-branch pipe use 1% to 2% isoflurane-oxygen mixture flow. In order to stimulate the tail veins, warm water held in a bottle was used directly on the mouse tail for a bit second. Then the tail was held on its upper end by middle and trigger finger to pond the venous blood, after injecting with the 30G cannula, the blood would pond out into the tube which means the cannula goes insides the vein, afterwards the syringe was connected and mfge-

8 was injected into the body slowly and evenly. After injecting with mfge-8, filled the tube with less than 50µl 0.9% NaCl to make sure none was left in the tube and all the mfge8 went into the tail vein. Then 30mins later, the mice were sacrificed, and organs were collected.

3. Flow Cytometry

3.1. Sample Preparation for Flow Cytometry

3.1.1. Cardiac Blood Withdrawal

The mouse was first anesthetized use MMF as mentioned above, placed on its back and fixed on a warm plate with adhesive tape. Followed by a skin incision at the level of the 2nd intercostal space, in which part of the skin was also removed by a sterile operation scissor. Using a 2ml syringe (BD Discardit II Becton Dickson GmbH, Franklin Lakes, USA) filled with 5 μ l heparin (heparin sodium 25,000, ratiopharm GmbH, Ulm) and a 27G cannula (BD Mikrolance, Becton Dickson GmbH, Franklin Lakes, USA), the heart was punctured at a 45 degree angle in the 2nd intercostal space. Then the blood was taken as fast as possible. 100 μ l of the blood was taken to test the blood leukocyte using the Sysmex counter.

3.1.2. Mouse Heart Perfusion

After the blood was taken, the mouse was killed by a neck dissection. The abdominal and chest cavities were then opened, and an incision was made in the liver. The animal was next perfused through a stab in the left ventricle using a 10 ml syringe filled with PBS and a 27G cannula. Approximately 20 ml PBS in total was injected into the heart until all the blood was replaced when the flow became clear.

3.1.3. Tissue Collection

After PBS perfusion, the whole abdominal and chest were opened in order to put aside all the other organs and fat tissues out of the body except aorta and heart. The heart was then carefully dissected out and put into the 15ml falcon

(Polypropylene Conical Tube, Falcon®, Corning Science, Mexico) and kept on ice.

3.1.4. Preparation of the Tissues

Half part of hearts was placed in the petri dish (TC dish 35, Standard, Sarstedt, Nümbrecht) and cut into 1-2 mm pieces using a scalpel (disposable safety blades, Aesculap AG, Tuttlingen) and tweezers. Then 4ml of the enzyme collagenase type IV (Gibco by life technologies, USA) were added in a concentration of 1µg/ml and samples were transferred to 50ml falcons. Then the samples were incubated for 30 mins at 37°C and 400rpm speed shaking (Thermomixer comfort, Eppendorf, Hamburg). In the next step, the samples were passed through a 70µm cell sieve (cell strainer: 70µm nylon, Falcon®, Corning, NY, USA) with a 6well plate (Costar 6 well plate, flat bottom, Corning, New York, USA), then transferred to a 15ml falcon.

Then all the hearts were centrifuged for 5mins at 350 x g (rcf) at 4°C, then the supernatant was aspirated, the left samples were transferred into a 96 well plate (Costar 96 well plate, flat bottom, Corning, New York, USA). Each heart sample was distributed into 3 wells with one well as a negative control. 50µl Fc block was added into each well of the samples, after 10mins incubation time on ice, the antibody mix was added 50µl per well. The subsequent incubation time was at least 20mins. Then 100µl flow cytometry buffer was added per well to wash and the plate was centrifuged at 350 x g (rcf) at 4°C for 5mins. The supernatant was poured off and the samples were resuspended with 200µl flow cytometry buffer. Before the samples were transferred to flow cytometry tubes, they were filtered through a 50µm sieve (Cell Trics 50µm, Sysmex Partec, Görlitz). The Cell Analyzer BD LSR Fortessa was used for the analysis of the samples.

4. Histological examination

4.1. Immunofluorescence staining

4.1.1. Organ Fixation

After anesthesia, mouse was sacrificed and perfused the same as mentioned above. After removal from the body, tissues were fixed in a 4% PFA solution for 30 min and then dehydrated in a 30% sucrose solution (Sigma-Aldrich, St. Louis, USA) overnight to prevent ice crystals in the subsequent freezing process. For this purpose, the hearts were embedded in cryo embedding molds (Tissue-Tek Cryomold 25 x 20 x 5 mm, Sakura Finetek) using an embedding medium (tissue-tek, Sakura Finetek Europe) and frozen on dry ice. For the I/R models, the hearts were cut into 3 parts horizontally in a wax pattern and kept separately. And the lowest part was applied for the immunohistology. For the other models, hearts were cut into two equal parts and saved. Then the tissues were placed in the freezer at -80°C before cut.

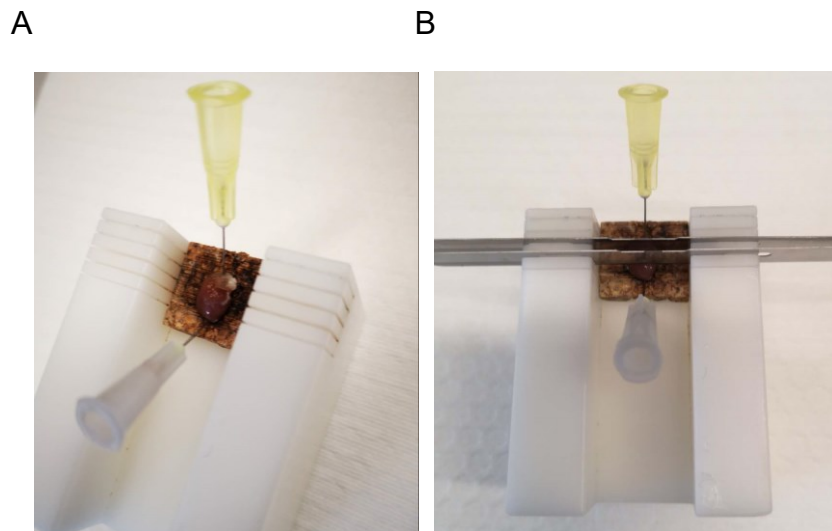


Figure 11 The indications of how to fix and cut hearts. The fixed heart on a wax pattern (A) and three parts of heart were cut equally with blades (B).

4.1.2. Frozen Heart Tissue Sections

Heart tissue was removed from the -80°C freezer and put into the cryotome (CryoStar NX70, Thermo Fisher Scientific), then after around 30 mins, tissue Tek was applied onto the cutting plate to solidify the heart in the chamber in order to cut. Make sure the heart tissue should stand vertically on the plate. Then 10µm thick sections were made at an interior temperature of - 18°C and a blade temperature of - 25°C. After four to six cuts, a trim cut of 50µm was carried out in order to examine the tissue from at least three different levels. If the cuts were not processed immediately, they were kept in storage boxes in the - 20°C freezer for longer storage.

4.1.3. Procedure of Immunofluorescence staining

First, the slides (Menzel glasses Superfrost Plus, Gerhard Menzel, Braunschweig) with the heart sections were warmed up for 10mins at room temperature. This was followed by fixation with 4% PFA for 10mins. The sections were then washed three times for 5 min each in a square staining jar with PBS-T (0.1% Tween20, Sigma-Aldrich Chemie GmbH, Steinheim). Now the tissues to be stained were encircled with a grease stick (Liquid Blocker, Science Service, Japan) and 50µl blocking solution per cut (PBS + 0.5% saponin (Sigma-Aldrich) + 1% BSA + 10% goat serum (Sigma-Aldrich)) applied to prevent non-specific bindings. After one hour, the blocking solution was poured off and the primary antibodies diluted in blocking solution were applied. These were incubated in a moist chamber for 1.5-2 hours at room temperature, protected from light. The slides were then rinsed with PBS-T three times for 5 mins each. In the next step, the secondary antibodies were used for core staining last for one hour at room temperature. The stock solution (PBS + 0.5% saponin and 1% BSA) served as the dilution medium.

As the lectin WGA (wheat germ agglutinin, Life Technologies) already coupled to a fluorochrome, so it was applied together with the secondary antibody. It was used to display fibrotic tissue in the heart, since it binds to sialic acid and N-acetylglucosamine residues, which are found in proteins in the extracellular matrix. After one hour, the secondary antibodies and WGA were poured off and the fluorescent dye Hoechst (Invitrogen) was used for 10mins. After a further washing step, the sections were wetted with mounting medium (Dako Fluorescence Mounting Medium, Dako North America Inc., USA), and covered with cover glasses (Menzel glasses, Thermo Scientific), then stored in the fridge at 4°C before observation.

During these mouse strains, the fibrosis was stained with WGA, the macrophages with CD68 (Rat, MCA1957, Bio-Rad), the mfg8-GFP with anti-GFP (Rabbit, Life Technologies), and the cell nuclei with Hoechst. In parallel, an isotype control for CD68 (Rat IgG2a Isotype Control, eBioscience) and one for anti-GFP (Rabbit Immunoglobulin Fraction Negative Control, Agilent Dako), as well as a negative control in which only the secondary antibody was applied.

4.2. Masson Goldner Trichome Staining

4.2.1. Paraffin-embedded Tissue Sections

After the aorta was taken from the mouse and put into the 4% PFA for 30 mins, the aorta was dehydrated and added into the molten paraffin wax. Steps are as followed. First, the tissue was immersed in 70% ethanol three times for 30 mins each at room temperature, then put in 90% ethanol twice for 30 mins each, last in 100% ethanol three times for 30 mins. In the end, immersed the tissue in xylene three times for 20mins each. Embedded the tissue in paraffin at 58°C. Aorta was embedded into paraffin with a professional mechanized tissue processing system. Before sectioning, paraffin-embedded aorta blocks were

chilled on ice first. The water bath was filled with ultrapure water and heated to 40-50°C. Then the blade was placed in the holder, and the paraffin block was inserted and orientated. 5µm thickness was set, and a few sections were cut first to ensure the positioning was correct. Then tweezers were used to pick up the sections, then float them onto the surface of the heated water in the water bath. The microscope slides were applied to take the sections out of the bath and stored in a slide rack.

4.2.2. Procedure of Masson Goldner Trichome Staining

Masson-Golder's trichrome staining kit (Art. No. 3459, ROTH) was used. It contains Hematoxylin solution A (Art. No. X906), Hematoxylin solution B (Art. No. X907), Golder's staining I (Art. No. 3469), Golder's staining II (Art. No. 3470), and Golder's staining III (Art. No. 3473). All steps were followed by the instructions and paraffin sections were applied.

First of all, deparaffinize and rehydrate via 100% alcohol, 95% alcohol and 70% alcohol. Then distilled water was used to wash. Mixed solution A+B at a ratio of 1:1 was used to stain the sections at max. 3 mins. Then washed with flowing tap water for 10 to 15mins. Followed with Goldner's stain I around 5 to 10mins, then rinsed with acetic acid solution 1% for 30 seconds. Afterwards stained with Golder's stain II until decolouration of connective tissue from 1mins up to 30mins. Then rinsed with acetic acid solution 1% for 30 seconds. Followed with counterstain with Goldner's stain III from 2 to 5mins. Washed with acetic acid solution 1% around 2 to 5mins. Last, sections were dehydrated by ascending alcohol series as mentioned above, and then mounted with mounting medium. All sections were kept at room temperature before examined by microscope.

4.3. Sirius Red / Fast Green staining

First, the frozen sections were used and kept at room temperature for at least

one hour. Then incubated them in pre-heated Bouin's Solution at 58°C for one hour. Washed the sections in running tap water in order to remove the yellow color around 10 to 15 mins. Then stained them in 0.1% Fast green (Fast Green FCF, Sigma-Aldrich) for 20 mins at room temperature. Rinsed in 1% acetic acid for one minute then discard solution, washed in tap water for 5mins. In the next step, sections were stained in 0.1% Sirius red (Direct Red 80, Sigma-Aldrich) for 30 mins. Afterwards, went to dehydrate, slides were put into 70% ethanol for 10 seconds, 100% ethanol for 1 minute and then 100% Toluol for 3mins. Last, covered the slides with DePex (Serva Electrophoresis GmbH) about 50µl each and put a coverslip on top. The slides were dried overnight at room temperature.

4.4. TUNEL assay

In this thesis, the ApopTag® Red In Situ Apoptosis Detection Kit (S7165, Sigma-Aldrich) was used. All steps were followed by the instructions. First, frozen sections were pretreatment with 0.2% Triton X-100 in PBS for 30mins. Then rinsed sections in 2 changes of PBS-T for 2mins each. Used the blocking solution to incubate sections for 10mins, then rinsed in PBS-T for 3 times and 2mins each. Then incubated sections in TdT reaction solution for 1 hour at 37°C in humidified chamber. Followed with Stop wash buffer for 10mins at room temperature, then rinsed in PBS-T 3 times and 2mins each. And then mounted with mounting medium.

4.5. Histological Evaluation

The colored sections were taken at 5,10, 20- or 40-times magnification on an epifluorescence microscope (Axio Imager.M2, Carl Zeiss, Jena) using a digital camera (AxioCam MRm, Carl Zeiss, Jena). The following filters were used to display the colorations: DAPI (BP: 445/50), GFP (BP: 525 / 50), Cy3 (BP: 605/70), Cy5 (BP: 690/50). In animals treated with ANG II, 6 images from three

different levels were analyzed for each heart. In the I/R mouse models, 6 images also taken at the infract area of each heart at 2 to 3 different levels. In the next step, 3 or 4 different area of the heart were selected and examined more detail in 40 times magnification both in fibrotic area and non-fibrotic area. The images were evaluated using Zeiss software (AxioVision SE64 Rel. 4.9.1). With the Zeiss software it was possible to determine the fibrosis area in the heart and to calculate the ratio of this to the entire heart area.

5. qPCR of mRNA levels

SsoAdvanced universal SYBR Green was used. All the frozen reaction components were thawed and then kept on ice protected from light. In order to collect contents at the bottom of tubes, they were mixed carefully and centrifuged briefly at 4°C. Afterwards necessary ingredients and samples were added into the reaction mixture tubes to a total volume by 20µl. Mixed the reaction components well and vortexed to avoid the air bubbles at the same time. Collected the reaction mixture and put the PCR tubes or plate onto the real-time PCR machine and lastly started the PCR run⁹³.

6. Statistical Analysis

The data collected was analyzed using the GraphPad Prism 5 software (GraphPad Software, Inc., Jolla USA). Microsoft PowerPoint (PowerPoint 2016 (Windows), Microsoft Corporation, Redmond, USA) was used to optimize the graphic display. Student's unpaired t-test was used for the comparison of two groups with significant differences. Error bar indicates standard deviation (SD). Statistical significance was considered when p value less than 0.05.

IV. Results

The focus of this thesis is investigating the role of Regnase-3 in cardiac macrophages in acute and chronic inflammation.

1. Regnase-3-deficient Mice at Steady State

1.1. Cardiac Fibrosis at Steady State

The quantification of fibrotic tissue is necessary in the cardiac remodeling. In order to investigate whether there is fibrosis formation in the Regnase-3-deficient mice during age, WGA (wheat germ agglutinin), which is used to detect cardiac fibrosis, was applied to the frozen heart sections of both Regnase-3 knockout-first allele mouse strain (around 6 months old) and Rosa26-Cre; Regnase-3^{fl/fl} mouse strain (around 2-3 months old). Their littermates were applied as control groups, both homozygotes and heterozygotes. The fibrosis percentage of heart cross section has no difference between wild type, heterozygotes and full knockout mice of Regnase-3^{-/-} mouse strain. There was also no difference between Regnase-3^{fl/fl} and Rosa26-Cre; Regnase-3^{fl/fl} group. This indicates that during age, the fibrosis formation of Regnase-3 knockout mice did not develop.

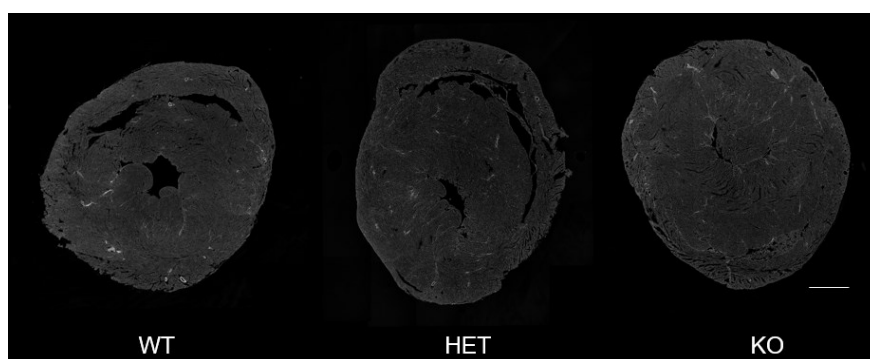


Figure 12 WGA staining of heart cross section from Regnase-3 knockout-first allele mice (around 6 months old) at steady state. Left to right, wild type, heterozygous and knockout genotype separately. Scar

no significance.

1.2. Cardiac Macrophage Number at Steady State

CD68 is highly expressed in macrophages/monocytes and widely used as a marker to detect them in many tissues. In this study, in order to find out whether there is number difference between wild type and knockout mice of Regnase-3^{-/-} mouse strain, anti-CD68 was applied to stain macrophages. We quantified the number of macrophages in the heart and found that in Regnase-3^{-/-} mouse strain, CD68⁺ number was not significant increased compared with HET group. And, there was no difference between groups of Rosa26-Cre; Regnase-3^{fl/fl} mouse line.

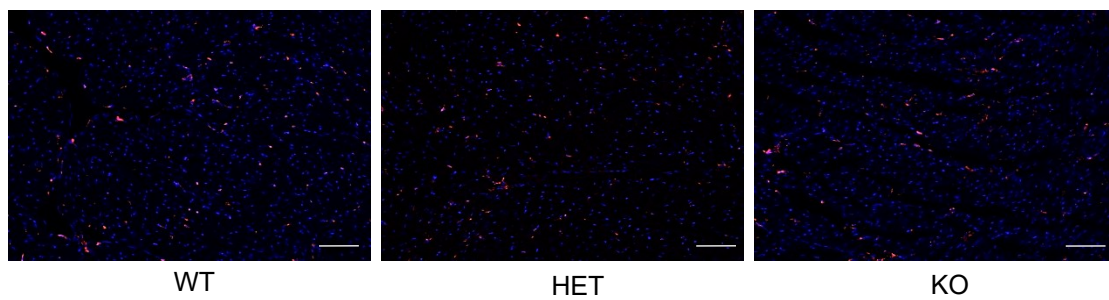


Figure 16 CD68 staining of heart cross section from Regnase-3 knockout-first allele mice (around 6 months old) at steady state. Left to right, wild type, heterozygous and knockout genotype separately. CD68, red. DAPI, blue. Scar bar, 200 μ m.

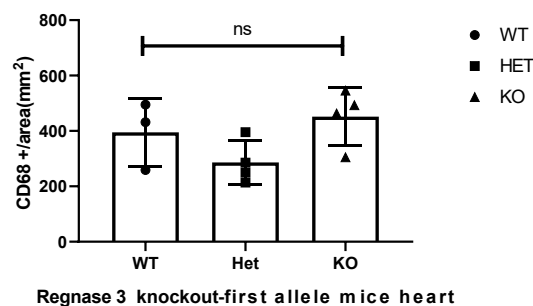


Figure 17 Quantification on heart CD68 staining of macrophages number from Regnase-3 knockout-first allele mice (around 6 months old) at steady state. WT group n=3, HET group n=4, KO group n=4. Unpaired t-test; error bar= SD. n. s.= no significance.

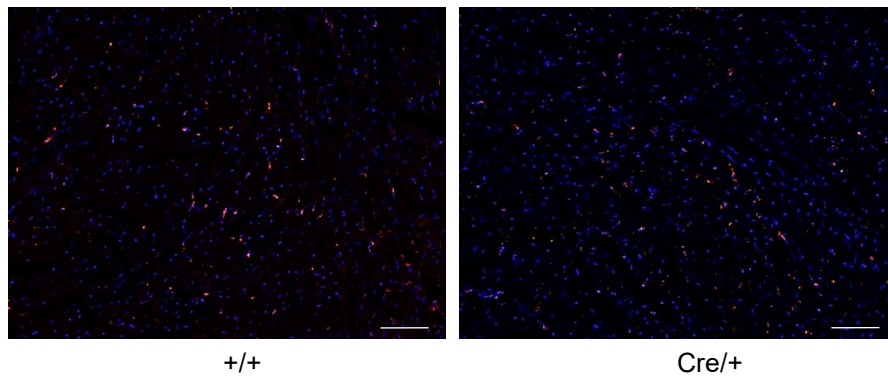


Figure 18 CD68 staining of heart cross section from Rosa26-Cre; Regnase-3^{fl/fl} mice (around 2 to 3 months old) at steady state. Genotype +/+ and cre/+ separately. CD68, red. DAPI, blue. Scar bar, 100µm.

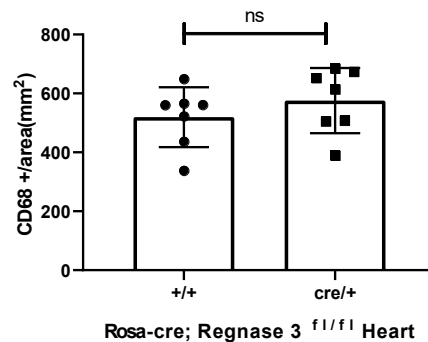


Figure 19 Quantification on heart CD68 staining of macrophages number from Rosa26-Cre; Regnase-3^{fl/fl} mice (around 2 to 3 months old) at steady state. n=7 in each group. Unpaired t-test; error bar= SD. n. s.= no significance.

1.3 Cardiac Inflammatory Factors at Steady State

In order to test whether there is change of inflammatory factors during aging at steady state of Regnase-3 deficient mice, the method of qPCR was applied to test the mRNA levels of the inflammatory chemokines and cytokines, including IL-6, interferon gamma (Ifng1), C-X-C motif chemokine 10 (Cxcl10), transforming growth factor beta 1 (Tgfb1), IL-1b, Regnase-1, IL-10 and signal transducer and activator of transcription 1 (Stat1). Both Regnase-3^{-/-} mouse strain and Rosa26-Cre; Regnase-3^{fl/fl} mouse line showed increased mRNA

levels of inflammation factors to some extent.

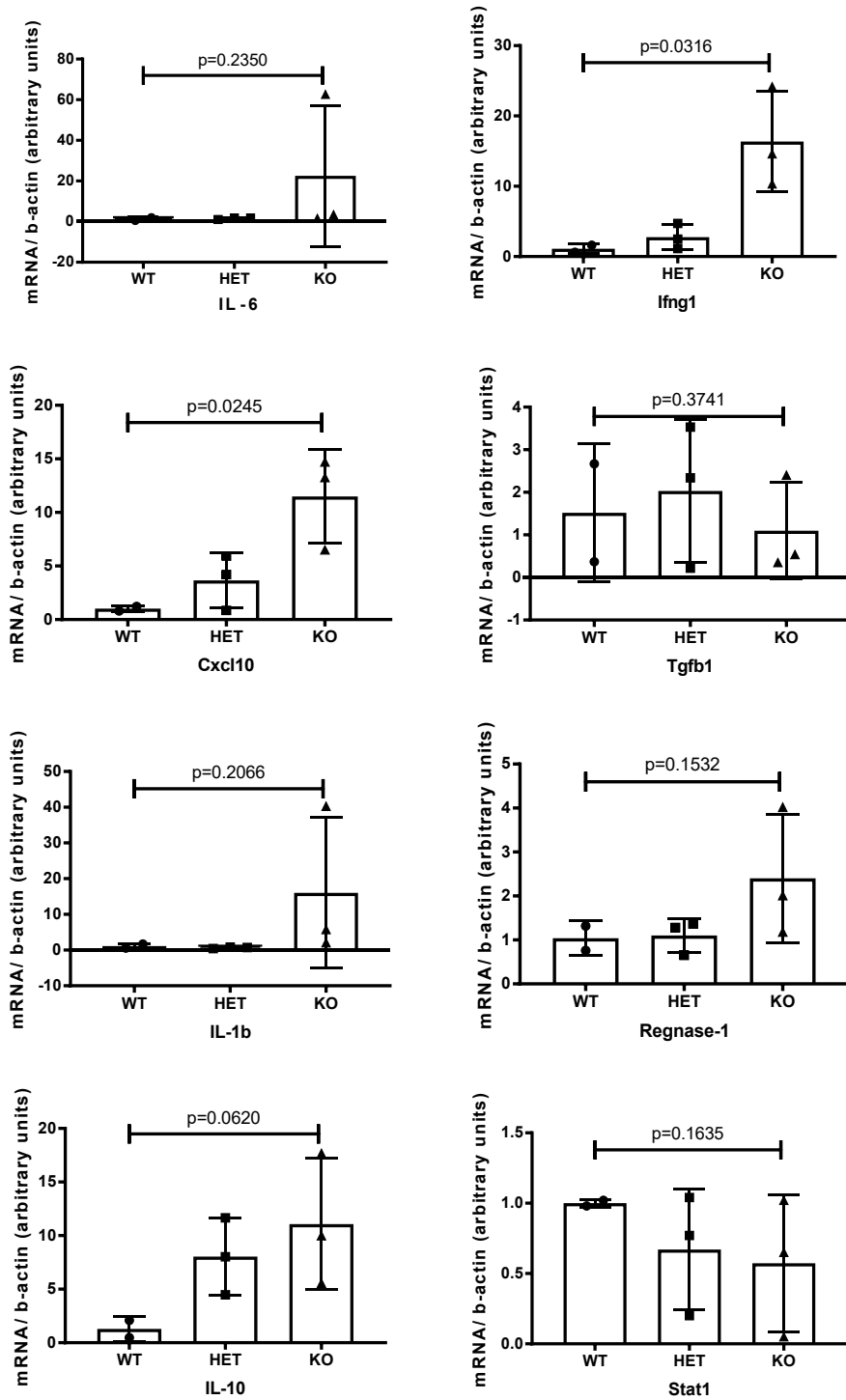


Figure 20 qPCR of cardiac tissue from Regnase-3 knockout-first allele mice (around 6 months old) at steady state. mRNA levels of IL-6, Ifng1, Cxcl10, Tgfb1, IL-1b, Regnase-1, IL-10 and Stat1 were shown separately. WT group n=2, HET group n=3, KO group n=3. Unpaired t-test; error bar= SD.

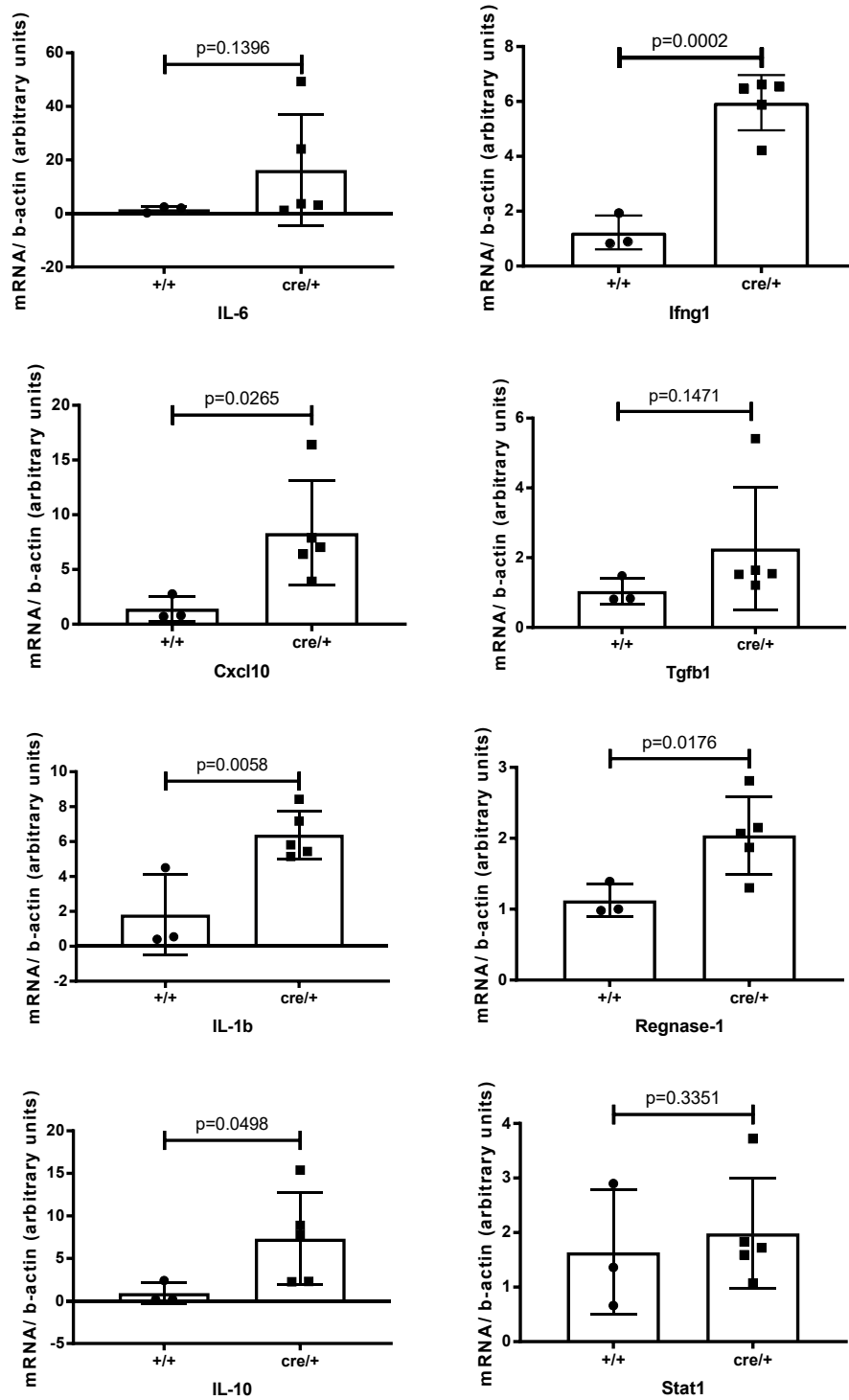


Figure 21 qPCR of cardiac tissue from Rosa26-Cre; Regnase-3^{fl/fl} mice (around 2 to 3 months old) at steady state. mRNA levels of IL-6, Ifng1, Cxcl10, Tgfb1, IL-1b, Regnase-1, IL-10 and Stat1 were shown separately. +/+ group n=3, cre/+ group n=5. Unpaired t-test; error bar= SD.

2 ANG II Mouse Models

2.1 LysM-Cre; Regnase-3^{fl/fl} mouse strain

2.1.1 Histological Evaluation of Adventitia Fibrosis

In order to investigate whether there is fibrosis formation in the LysM-Cre; Regnase-3^{fl/fl} mouse line after 10 days ANG II pump implantation, Masson Goldner Trichome staining was applied to the aorta paraffin sections. The littermates were used as control group. The green color showed the fibrosis formation in the adventitia, however there was no significant difference between littermates and LysM-Cre group.

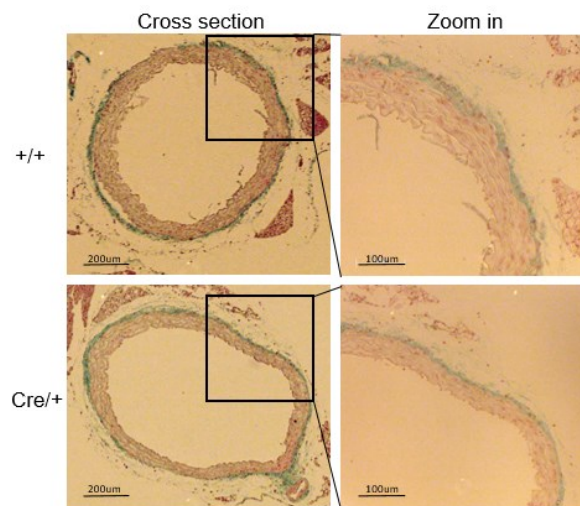


Figure 22 Masson Goldner Trichome staining of aorta cross section from LysM-Cre; Regnase-3^{fl/fl} mice heart after 10 days ANG II pump implantation. Top to bottom, genotype +/+ and cre/+ are shown separately. Left to right, whole cross section and zoom in separately, scale bar, 200um and 100um separately.

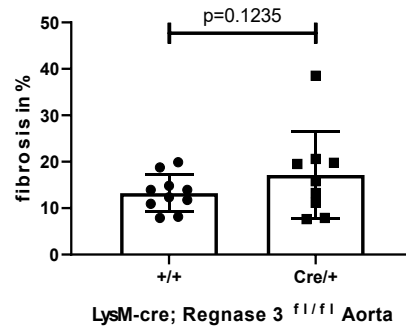


Figure 23 Quantification on Masson Goldner Trichome staining of fibrosis from LysM-Cre; Regnase-3^{fl/fl} mice heart after 10 days ANG II pump implantation. Regnase-3^{fl/fl} group n=10. LysM-Cre; Regnase-3^{fl/fl} group n=9. Unpaired t-test; error bar= SD. n. s.= no significance.

2.1.2 Histological Evaluation of Cardiac Fibrosis

In order to determine the fibrosis percentage of the heart cross section after 10 days of ANG II treatment, WGA staining was used to the LysM-Cre; Regnase-3^{fl/fl} mouse strain. Compared with the control group, the fibrosis percentage was increased after treatment. This indicated that the Regnase-3 ablation in myeloid lineage develop more fibrosis formation after ANG II treatment.

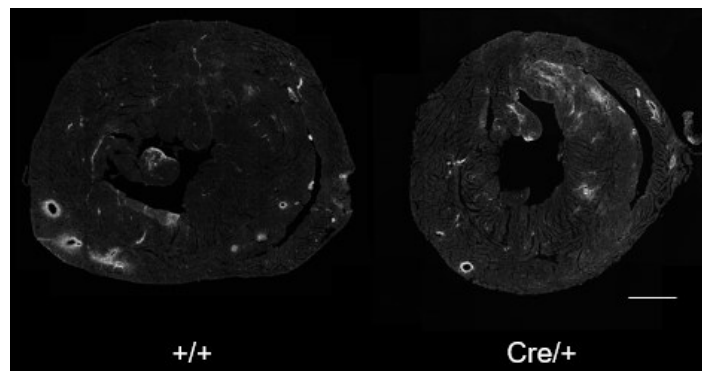


Figure 24 Heart WGA staining of LysM-Cre; Regnase-3^{fl/fl} mice after 10 days ANG II pump implantation. Genotype +/+ and cre/+ separately. Scar bar, 1000 μ m.

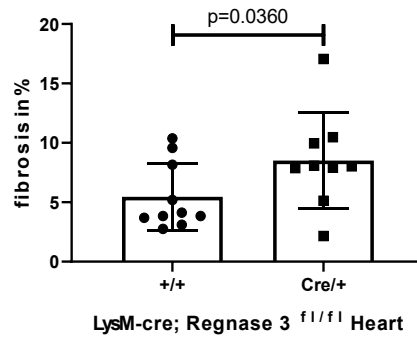


Figure 25 Quantification on WGA staining of fibrosis ratio from LysM-Cre; Regnase-3^{fl/fl} mice heart after 10 days ANG II pump implantation. Regnase-3^{fl/fl} group n=10. LysM-Cre; Regnase-3^{fl/fl} group n=9. Unpaired t-test; error bar= SD. P= 0.0360.

2.1.3. Cardiac Macrophages Quantification after ANG II treatment

An antibody to detect CD68 was used to stain macrophages as mentioned above. After ANG II treatment, fibrotic area and remote area were both tested, however there was no significant difference compared with littermate group. This indicated that after pump implantation, the CD68+ number had no changes neither at fibrosis area nor at remote area.

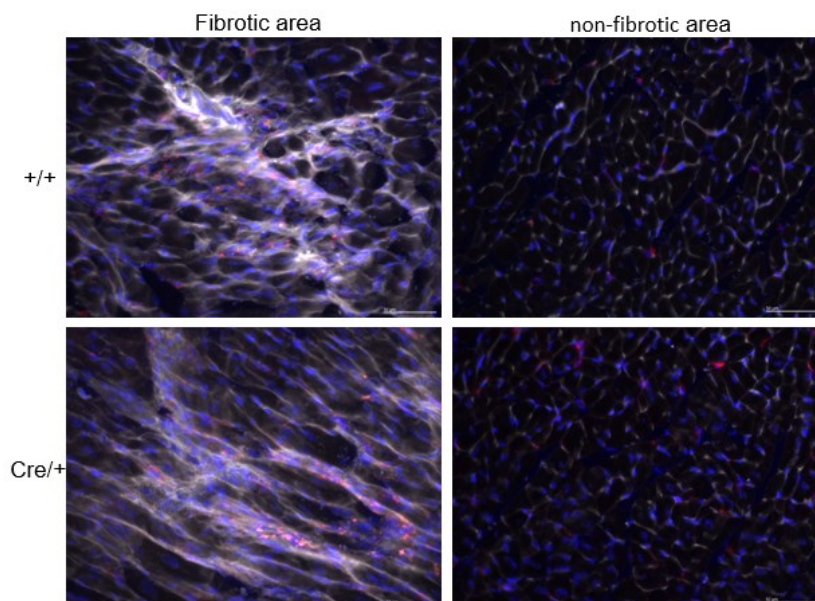


Figure 26 Heart WGA and CD68 staining of LysM-Cre; Regnase-3^{fl/fl} mice after 10 days ANG II pump implantation. Left to right, fibrotic area and un-fibrotic area separately. Up to bottom, genotype +/+ and cre/+ separately. WGA, white. CD68, red. DAPI, blue. Scar bar, 50µm.

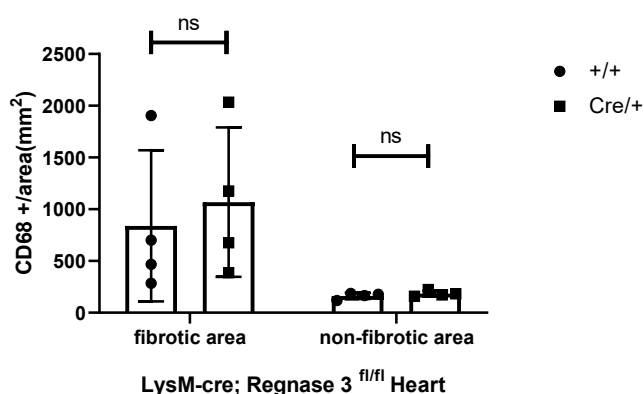


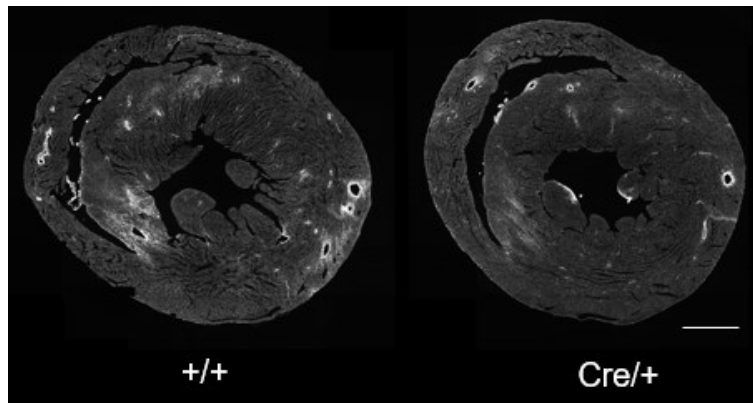
Figure 27 Quantification on CD68+ cells from LysM-Cre; Regnase-3^{fl/fl} mice hearts after 10 days ANG II pump implantation, fibrosis area and un-fibrosis area shown respectively. n=4 in each group. Unpaired t-test; error bar= SD. n. s.= no significance.

2.2. Rank-Cre; Regnase-3^{fl/fl} mouse strain

2.2.1. Histological Evaluation of Cardiac Fibrosis

As was previously shown that the cardiac fibrosis was increased after pump implantation of Regnase-3 ablation in myeloid lineage, therefore we want to know that if there is also difference of Regnase-3 ablation in tissue-resident macrophages. In order to make it more comparable, both WGA and Sirius red/fast green staining were applied to the Rank-Cre; Regnase-3^{fl/fl} mouse strain after ANG II treatment. These two methods are both suitable for the cardiac fibrosis. Interestingly, we found that after ANG II treatment, cardiac fibrosis was decreased compared with littermates. This indicated that after deletion Regnase-3 in tissue-resident macrophages, the cardiac fibrosis was attenuated.

A



B

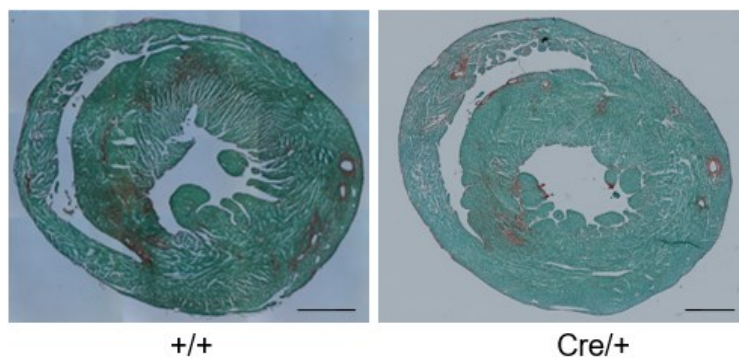
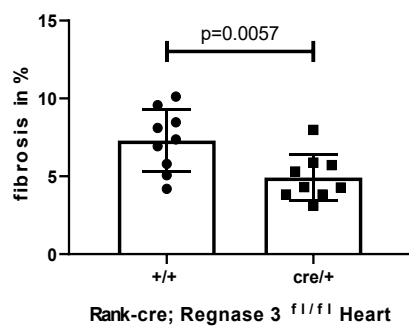


Figure 28 Heart WGA (A) and fast green/sirius red (B) staining of Rank-Cre; Regnase-3^{fl/fl} mice after 10 days ANG II pump implantation. Genotype +/+ and cre/+ separately. Scar bar, 1000µm.

A



B

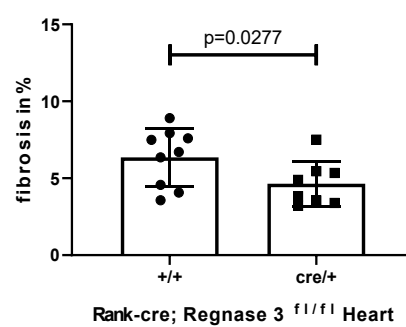


Figure 29 Quantification of both WGA (A) and Sirius red/fast green (B) staining of fibrosis ratio from Rank-Cre; Regnase-3^{fl/fl} mice heart after 10 days ANG II pump implantation. Regnase-3^{fl/fl} group n=9. Rank-Cre; Regnase-3^{fl/fl} group n=8. Unpaired t-test; error bar= SD. P=0.0057 (WGA). P=0.0277 (Sirius red/fast green).

2.2.2 Flow Cytometry Evaluation after ANG II treatment

In order to determine what how much frequency and how many macrophages and other immune cells were, a flow cytometry analysis of the heart was carried out. After 10 days ANG II treatment, the hearts were then removed and divided into the heart base and heart apex. The apex of the heart was prepared and analyzed for flow cytometric analysis. Flow cytometry analysis showed that except Ly6C⁺ cells, there was no significant difference of other immune cells compared with littermate group after 10 days infusion.

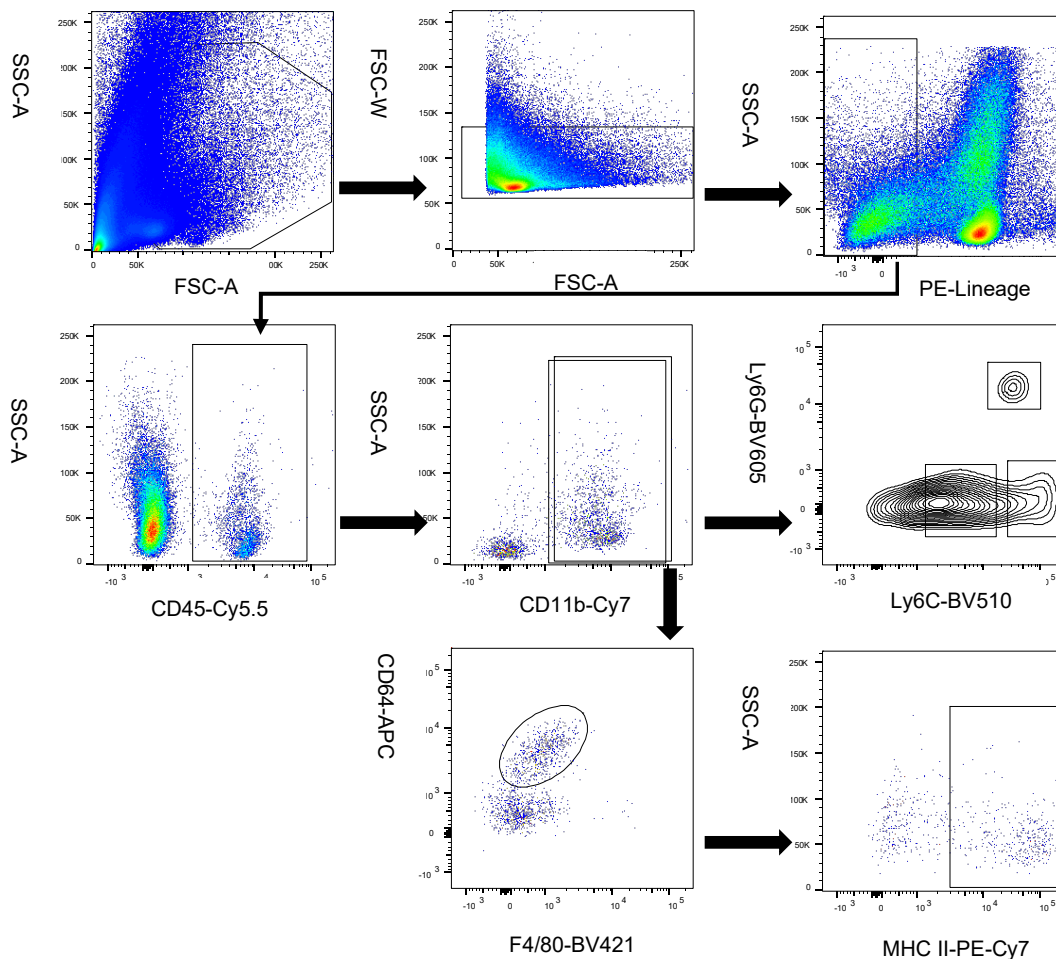


Figure 30 Representative flow cytometry plot of the heart of Rank-cre; Regnase-3^{fl/fl} mice after ANG II infusion. Exclusion of cell fragments a cell duplicates using the SSC and FSC. Identification of leukocytes (CD45⁺ cells). Cell lineage negative (PE negative cells, including NK1.1⁺, Ter119⁺ and dead cells). Check cell for expression of myeloid cells (CD11b⁺ cells), macrophage markers (CD68⁺, F4/80⁺ cells), neutrophils (Ly6G⁺ cells), monocytes (Ly6C⁺ cells) and MHC II⁺ cells.

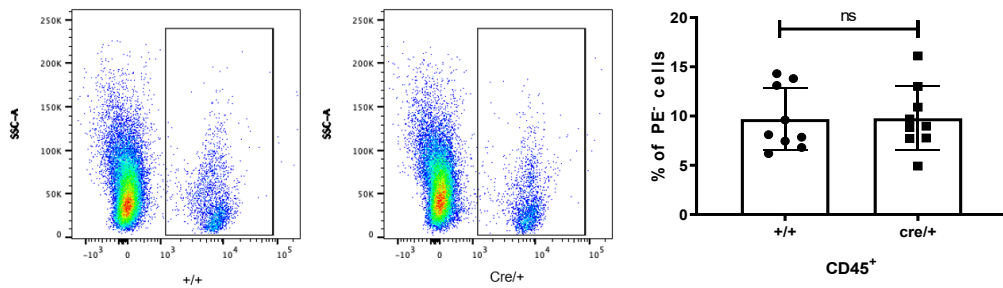


Figure 31 Frequency of leukocytes (CD45⁺ cells) in both Rank-Cre; Regnase-3^{fl/fl} mice and littermate controls assessed by flow cytometry (n=9) after 10 days ANG II treatment. Unpaired t-test; error bar= SD. n. s.= no significance.

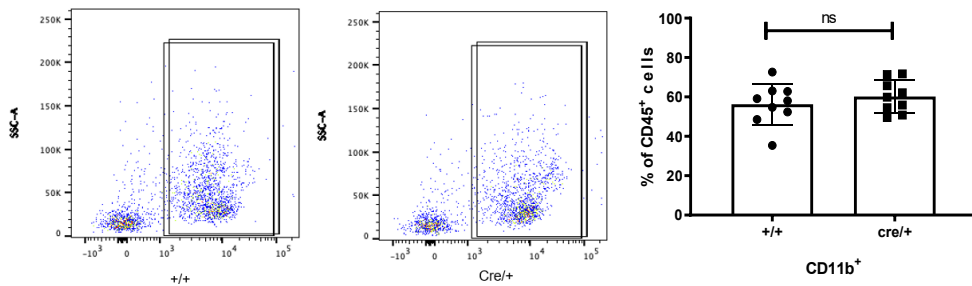
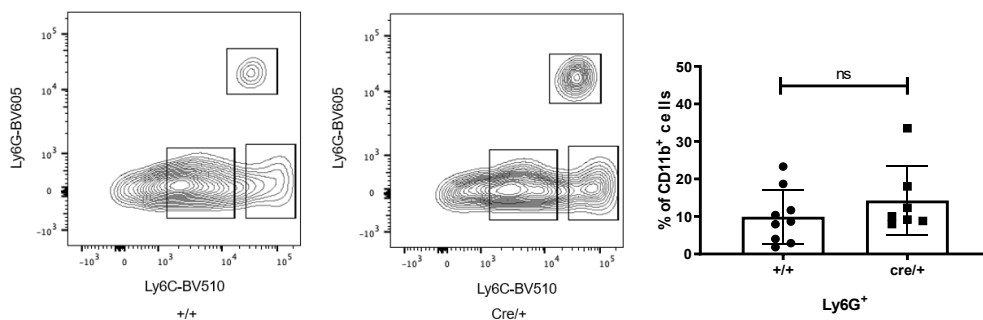


Figure 32 Frequency of myeloid cells (CD11b⁺ cells) in both Rank-Cre; Regnase-3^{fl/fl} mice and littermate controls assessed by flow cytometry (n=9) after 10 days ANG II treatment. Unpaired t-test; error bar= SD. n. s.= no significance.



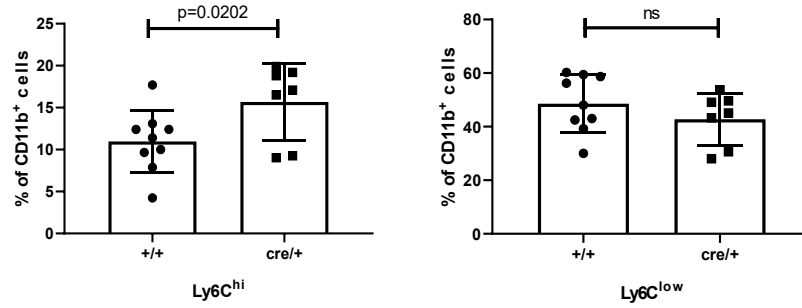


Figure 33 Frequency of neutrophils (Ly6G⁺ cells), inflammatory monocytes (Ly6C^{hi} cells) and non-classical monocytes (Ly6C^{lo} cells) in both Rank-Cre; Regnase-3^{fl/fl} mice and littermate controls assessed by flow cytometry (n=9) after 10 days ANG II treatment. Unpaired t-test; error bar= SD. n. s.= no significance.

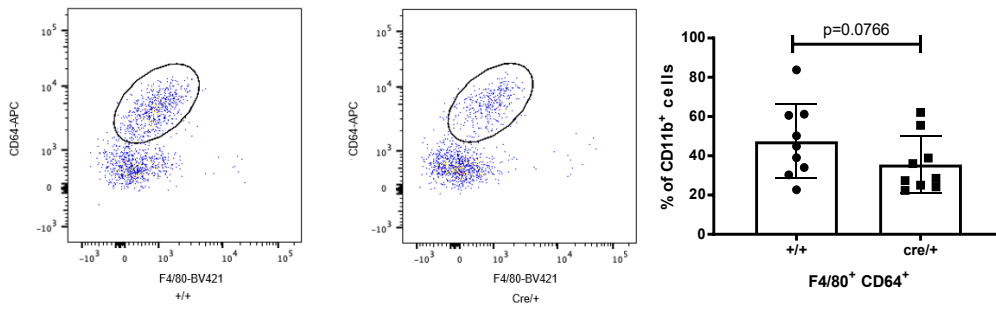


Figure 34 Frequency of macrophages (F4/80+ and CD64+ cells) in both Rank-Cre; Regnase-3^{fl/fl} mice and littermate controls assessed by flow cytometry (n=9) after 10 days ANG II treatment. Unpaired t-test; error bar= SD. P=0.0766.

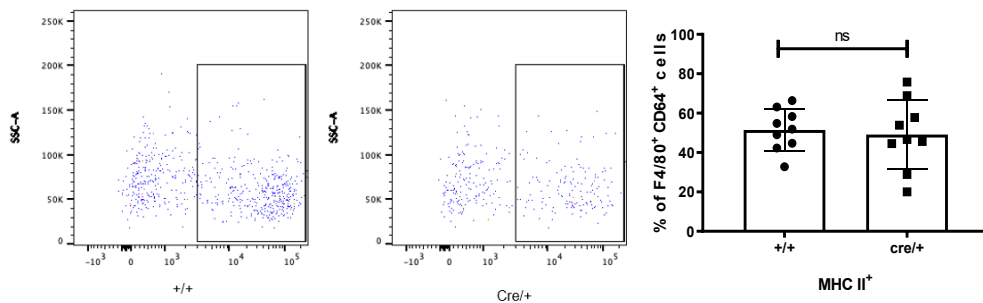
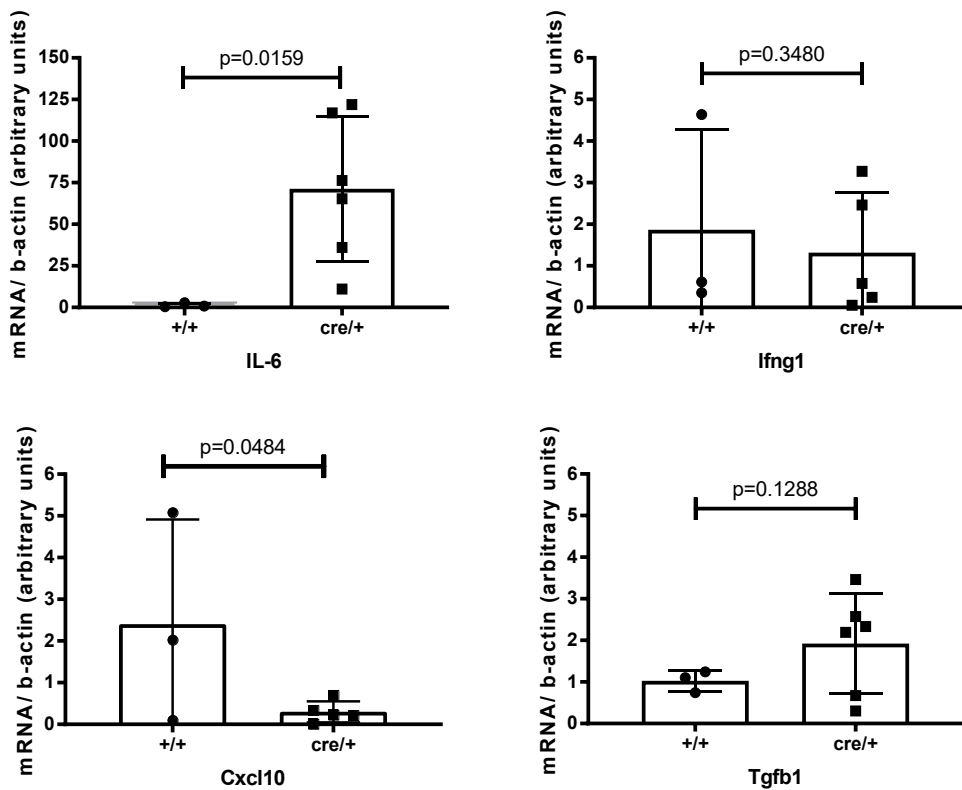


Figure 35 Frequency of MCH II⁺ cells in both Rank-Cre; Regnase-3^{fl/fl} mice and littermate controls assessed by flow cytometry (n=9) after 10 days ANG II treatment. Unpaired t-test; error bar= SD. n. s.= no significance.

2.2.3 Cardiac Inflammatory Factors after ANG II treatment

As mentioned above, the inflammatory factors changed during steady state of Regnase-3 deficient mice, in order to check whether it is the same after ANG II treatment of Rank-Cre; Regnase-3^{fl/fl} mouse strain, the method of qPCR was also applied to test the mRNA levels of the inflammatory chemokines and cytokines, including IL-6, Ifng1, Cxcl10, Tgfb1, IL-1b, Regnase-1, IL-10 and Stat1.



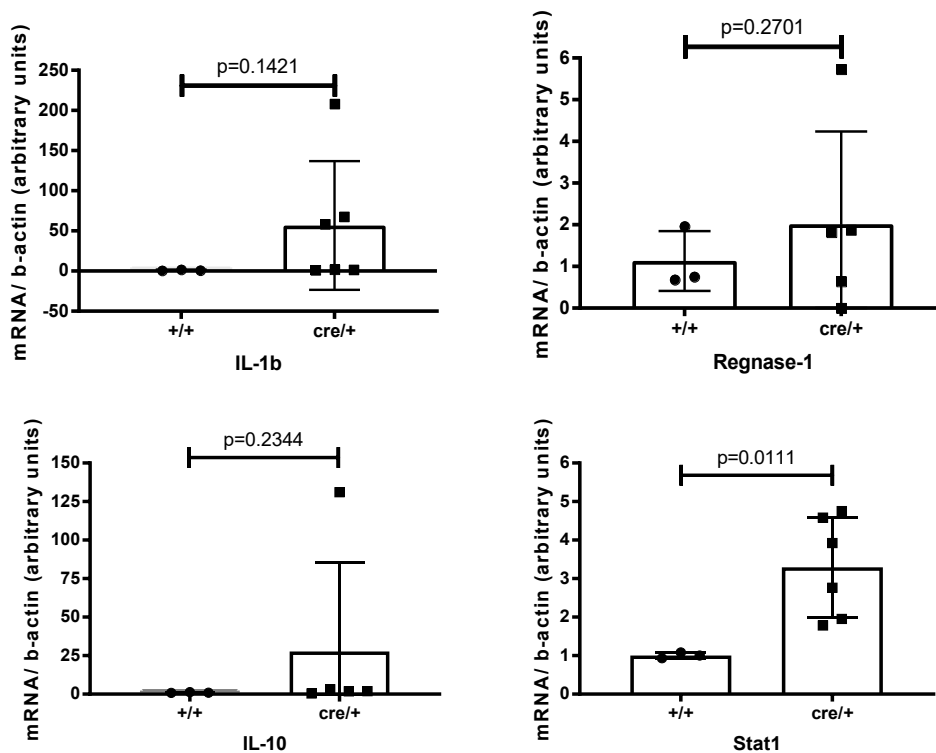


Figure 36 qPCR of cardiac tissue from Rank-Cre; Regnase-3^{fl/fl} mice after ANG II treatment. mRNA levels of IL-6, Ifng1, Cxcl10, Tgfb1, IL-1b, Regnase-1. IL-10 and Stat1 were shown separately. +/+ group n=3, cre/+ group n=5-6. Unpaired t-test; error bar= SD.

3. Ischemia Reperfusion Injury Mouse Models

3.1. Mfge-8 efficacy to Detect Apoptosis

Since mfge-8 was produced to detect apoptosis cells in vivo, C57BL/6J mouse strain was used to identify its efficacy. After injection mfge-8-GFP for 30mins, mice were sacrificed and hearts were collected to prepare immunofluorescent staining with purified anti-GFP and AF 488 as the secondary antibody. We first collected I/R mouse models at different time points, direct (0hour), 2hour, 6hour, 24hour, 48hour and day 7, to quantify the GFP percentage of heart cross section area. As shown, at 2hour and 6hour, the GFP ratio is higher than other time points, meanwhile the percentage decreased over time and became none after one week.

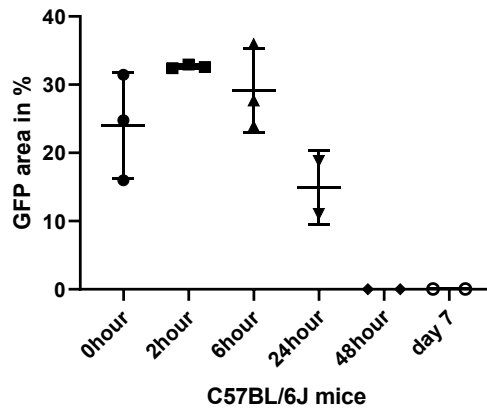


Figure 37 Quantification of mfge8-GFP area percentage of heart cross section area from C57BL/6J mice heart after ischemia reperfusion injury at different time points. n=2-3.

Then we try to figure out how much area were apoptotic cells, so we choose the 2hour time point heart to co-stain with TUNEL assay, at the same time we also did a sham group. Since the mfge-8 binds to the surface of the apoptotic cells and TUNEL is intracellular, we found that it's impossible to see a 1:1 overlap, however from the images, we could see in areas of lots of TUNEL, which makes mfge-8 a good reagent to detect the apoptosis in vivo.

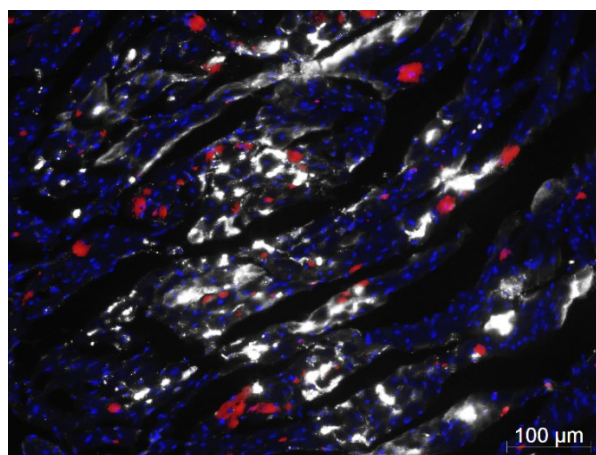


Figure 38 TUNEL and mfge8 co-staining. TUNEL, red. Mfge8, white. DAPI, blue. Scar bar, 100μm.

3.2. LysM-Cre; Regnase-3^{fl/fl} mouse strain

3.2.1. Apoptotic Area at I/R 6hour Time Point

6hour time point was chose to perform I/R injury on LysM-Cre; Regnase-3^{fl/fl} mice and their littermates as control group. 30 mins before mice were sacrificed, mpeg-8-GFP was injected into mice through tail vein. However, it showed no significant difference between groups. Interestingly, we could see a strong trend that after Regnase-3 ablation in myeloid lineage, the apoptotic area increased in I/R models.

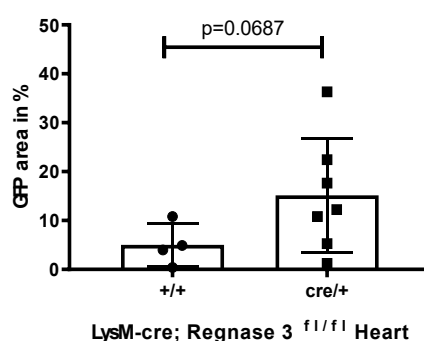


Figure 39 Quantification of GFP percentage of heart cross section area from LysM-Cre; Regnase-3^{fl/fl} mice heart after ischemia reperfusion injury at 6hour time points. Regnase-3^{fl/fl} group n=4. LysM-Cre; Regnase-3^{fl/fl} group n=7. Unpaired t-test; error bar= SD. P= 0.0687.

3.3. Rank-Cre; Regnase-3^{fl/fl} mouse strain

3.3.1. Peripheral Blood Counts after I/R Injury at Day 7 Time Point

Since macrophage has very important role in the cardiac healing and remodeling, we try to figure out whether there is difference after 7 days I/R injury compared with littermate group. Peripheral blood was counted at Day 7 after I/R injury, white blood cells, red blood cells, hematocrit, platelet, monocyte numbers and percentages were not altered in Rank-Cre; Regnase-3^{fl/fl} mice

compared with the littermate controls.

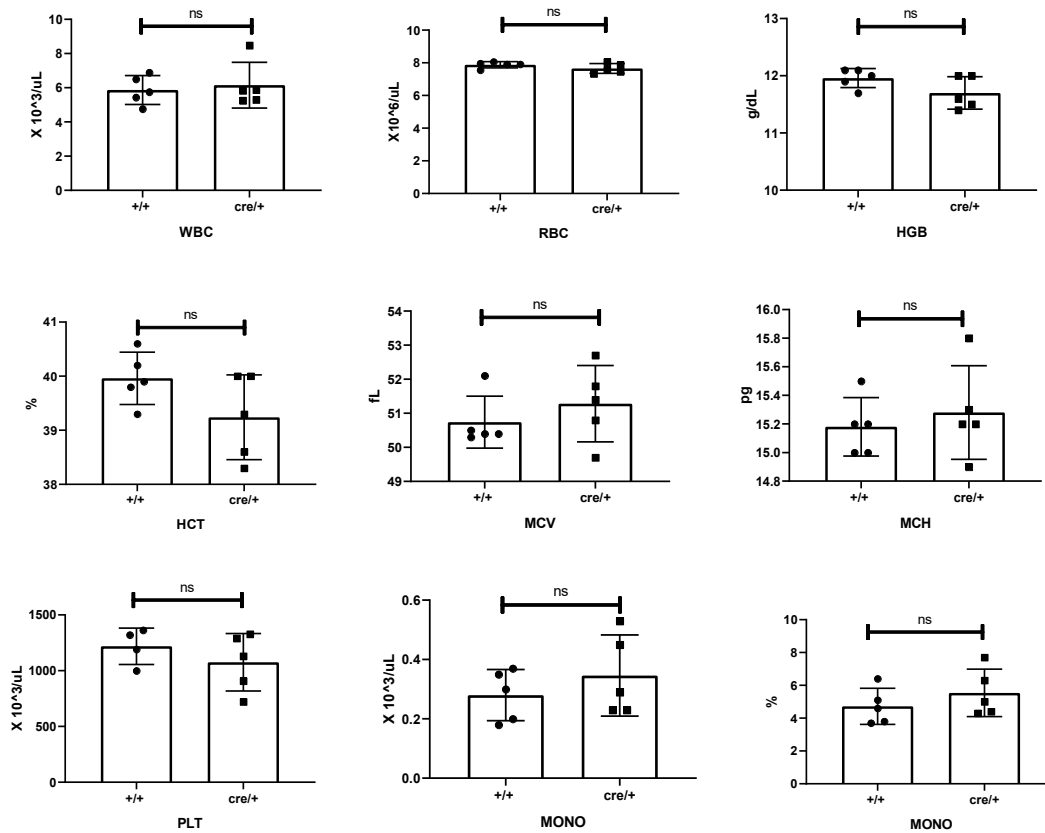


Figure 46 Peripheral blood counts in Rank-Cre; Regnase-3^{fl/fl} mice and littermate controls (n=5) after I/R injury at day 7. WBC, white blood cells; RBC, red blood cells; HGB, hemoglobin; HCT, hematocrit; MCV, mean corpuscular volume; MCH, mean corpuscular hemoglobin; PLT, platelets; MONO, monocytes. Unpaired t-test; error bar= SD. n. s.= no significance.

3.3.2. Cardiac Fibrosis at Day 7 Time Point

WGA staining was applied to the Rank-Cre; Regnase-3^{fl/fl} mice strain to figure out whether there is difference after 7 days I/R injury compared with littermate group. The quantification of fibrosis percentage showed no statistical difference between groups, which indicated that the Regnase-3 ablation of tissue-resident macrophages did not affect cardiac remodeling after 7 days of I/R injury.

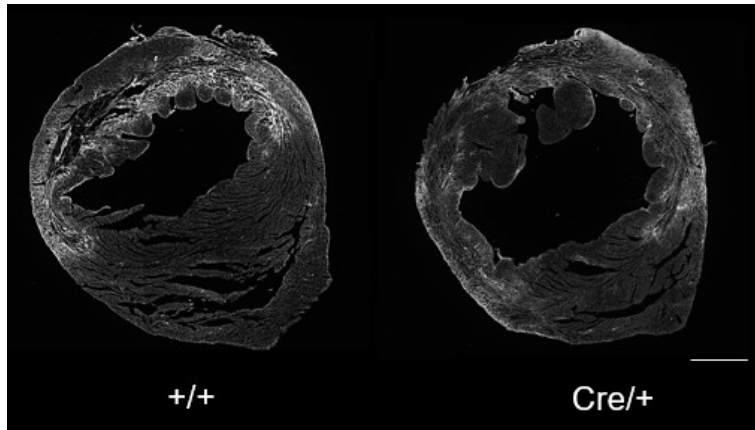


Figure 41 Heart WGA (white) staining of Rank-Cre; Regnase-3^{fl/fl} mice after I/R injury at day 7. Genotype +/+ and cre/+ separately. Scar bar, 1000μm.

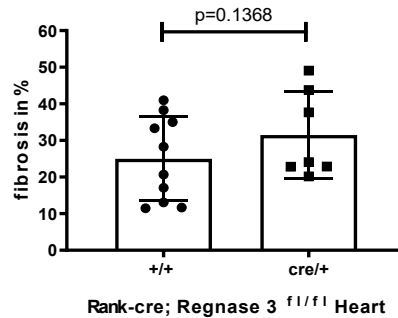


Figure 42 Quantification of WGA staining of fibrosis percentage from Rank-Cre; Regnase-3^{fl/fl} mice heart at Day7 of ischemia reperfusion injury. Regnase-3^{fl/fl} group n=10. Rank-Cre; Regnase-3^{fl/fl} group n=7. Unpaired t-test; error bar= SD. P=0.1368.

3.3.3. Cardiac Macrophages Quantification after I/R Injury

An antibody to detect CD68 was applied to stain macrophages as mentioned above. After I/R treatment, infarct area and remote area were both tested, however there was no significant difference compared with littermate group. This indicated that after I/R injury, the CD68+ number had no changes neither at infarct area nor at remote area.

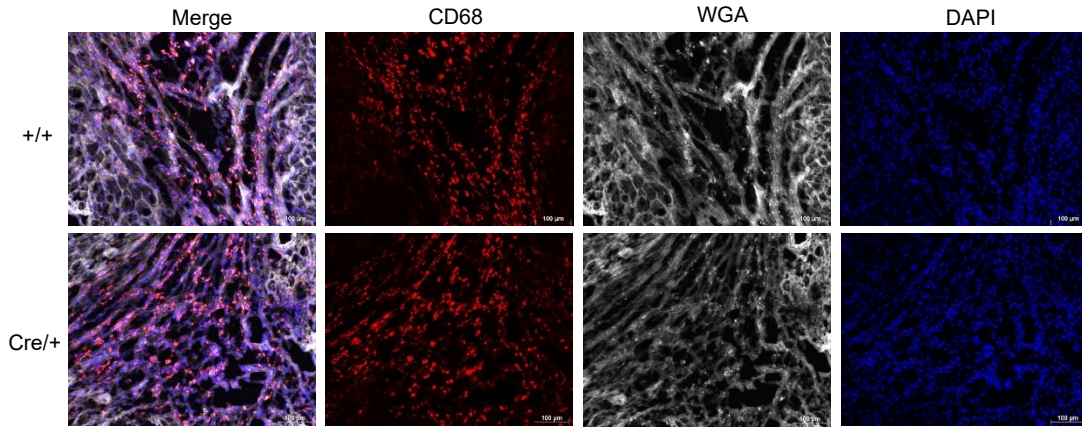


Figure 43 Heart WGA, CD68 and DAPI staining of Rank-Cre; Regnase-3^{fl/fl} mice at Day7 of ischemia reperfusion injury at infarct area. Left to right, merge, CD68, WGA and DAPI separately. Up to bottom, genotype +/+ and cre/+ separately. WGA, white. CD68, red. DAPI, blue. Scar bar, 100μm.

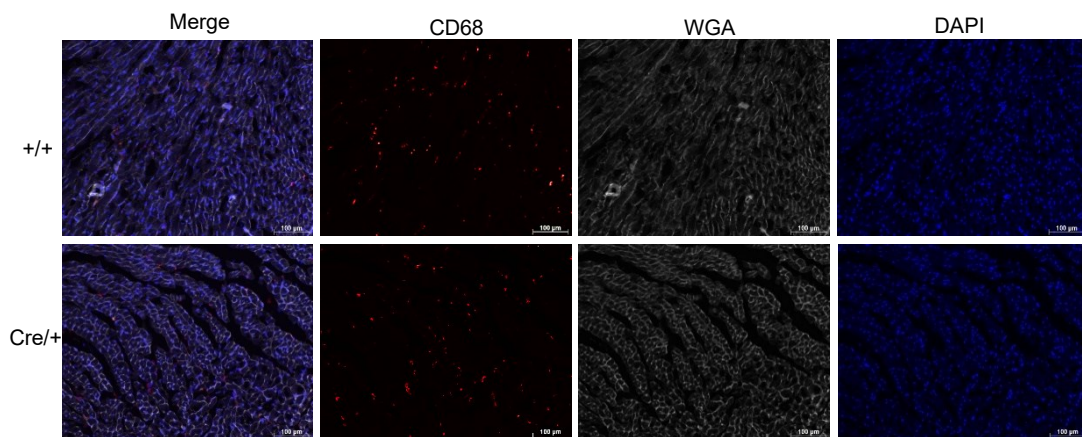


Figure 44 Heart WGA, CD68 and DAPI staining of Rank-Cre; Regnase-3^{fl/fl} mice at Day7 of ischemia reperfusion injury at remote area. Left to right, merge, CD68, WGA and DAPI separately. Up to bottom, genotype +/+ and cre/+ separately. WGA, white. CD68, red. DAPI, blue. Scar bar, 100μm.

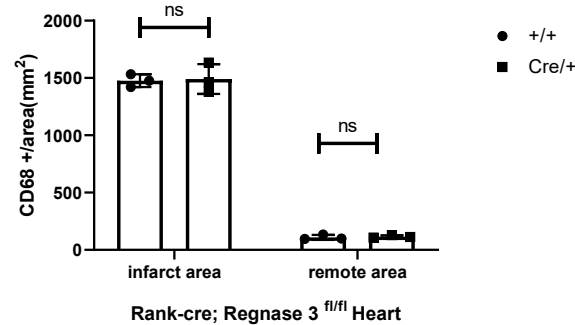


Figure 45 Quantification on CD68+ cells from Rank-Cre; Regnase-3^{fl/fl} mice at Day7 of ischemia

reperfusion injury at infarct and remote area shown respectively. n=3 in each group. Unpaired t-test;
error bar= SD. n. s.= no significance.

V. Discussion

The aim of this work was to investigate the role of macrophage Regnase-3 in acute and chronic inflammatory and fibrosis processes of the heart. The results and the knowledge gained from them should contribute to the development of new therapeutic strategies for cardiac diseases.

1. Mouse Model Methodology

In the ANG II infusion mouse models, we applied 10 days of osmotic pumps filled with ANG II and carried out histological examination and flow cytometry analysis of fibrosis and macrophages. This established chronic ANG II infusion model is widely utilized to induce hypertension and cardiac hypertrophy in mice^{40,48,57,94}. 4 weeks infusion of ANG II always applied to observe renal injury and damage with the measurement of blood pressure, as our experiment focus more on the process of cardiac hypertrophy, 10 days of infusion is efficient to study inflammation and fibrosis formation in mice heart. Model establishment was identified by fibrotic histology afterwards.

In the myocardial infarction mouse models, the widely used occlusion of the LAD is permanent with the confirmation by electrocardiogram showing the elevated ST segment^{23,83,89,95}, however, in order to make it more transferable to human patients in clinical situations, the ischemia reperfusion was chosen in our experiment instead of a permanent ligation of LAD. The successful infarction was confirmed by the paleness of anterior LV wall and arrhythmia, and was followed by one-hour ligation, reperfusion and chest closed. The mfg8 and WGA staining afterwards at different time points also confirmed successful myocardial infarction during the surgery.

2. Efficiency of Depleting Macrophage Regnase-3

LysM-Cre mouse strain was widely used to study the function of macrophages, monocytes and granulocytes as they express lysozyme M when activated^{96,97}. Clare L and colleagues found that LysM-Cre; ROSA-EYFP mice show ~50-70% recombination in neutrophils⁹⁸, which LysM-Cre mice were applied in our experiment, the depletion efficiency of myeloid Regnase-3 was also the same. The reason why we chose LysM-Cre to cross with Regnase-3 flox mice was that there is little expression of Regnase-3 in neutrophils, that makes it specifically depletion of myeloid-derived Regnase-3 in only monocytes and macrophages³⁶.

For the Rank-Cre mouse line which was gained from Kobayashi of Japan, ~80% of tissue resident macrophages were labeled in the Rank-Cre; Rosa26^{LSL-YFP} mice as well as ~15% of HSCs and HSC-derived cells in blood¹⁹.

3. The Identification of Fibrosis

As was mentioned above that Regnase-3 could be related to degrading extracellular material because of its localization and little change in gene expression³⁶, moreover during inflammatory reactions, a continuous deposition of components of the extracellular matrix, such as hyaluronic acid, fibronectin, proteoglycans and collagen, has a high relevant with fibrosis formation^{52,99}, hence we want to explore that whether Regase-3 deficient in macrophages would have any effect in fibrotic tissues in mouse models with cardiac diseases.

Masson trichrome stain is widely used in the aortic and cardiac sections in ANG II infusion models and MI models in order to detect perivascular fibrosis and cardiac injury^{48,57,100,101}. So, in our study, this method was applied to quantify the fibrosis percentage in the adventitia of aortas in the ANG II infusion models

after 10 days. Fibrosis was shown clearly in green color compared with other tissues which makes it an easier way to do the quantification. However, in our study of LysM-Cre; Regnase-3^{fllox} mice line, no significant different was shown between knockout group and littermates. So, in the next step we turn into the cardiac fibrosis.

WGA has the ability to co-immunostaining with other antibodies¹⁰². However, little was reported about WGA using in ANG II infusion models. So, in our experiments, we applied both methods in the ANG II infusion models to detect cardiac fibrosis after 10 days for the sake of verifying the consistency between WGA and Sirius red fast green staining. The results showed the fibrosis percentages were parallel in both methods, which means WGA is also valid in quantifying fibrosis in ANG II infusion models and we could take advantage of it to co-stain with other antibodies especially CD68 and DAPI.

4. Regnase-3 Deficient Mice at Steady State

RNA-binding proteins have the ability to regulate mRNAs at post-transcriptional level by recognizing RNA regulatory motifs or regions of secondary structures. Only small number (~2%) of RNA-binding proteins are tissue specific, the other are not, but they most bind at defined binding sites in cells¹⁰³. Regnase-1 was reported as an RNA binding protein and essential for the maintenance of immune system and mRNA degradation during inflammatory process as well as Roquin¹⁰⁴. Thus, we wonder as the same Regnase family member, whether Regnase-3 has the same or similar capacity under inflammation.

Regnase-3^{-/-} mice was reported leading to increased IFN signaling at steady state around 5 to 6 months old, and the expression of IFN- γ , MHC-II and Stat1 were increased without systemic autoimmunity but lymphadenopathy³⁶. In our Regnase-3 deficient mouse strains, both Regnase-3^{-/-} and Rosa26-Cre;

Regnase-3^{fl/fl} mice showed increased expression of IFN- γ in cardiac tissue, from 2 month to 6 months old, these results were in consistent with the previous findings from von Gamm et al that of serum cytokines. Besides, we also noticed that at steady state, the qPCR level of Cxcl10 was also increased compared with littermate controls in both mouse lines. At the same time, IL-1b, Regnase-1 and IL-10 were also increased in the Rosa26-Cre; Regnase-3^{fl/fl} mouse strain. However, in time of immunohistology with WGA staining, no significant increased fibrosis was detected in both mouse strains at steady state. Moreover, the number of macrophages in cardiac tissue also has no significant difference.

Acting as a RNase, Regnase-3 was reported to regulate macrophage activation³⁰, being involved in new genetic determinates of psoriasis¹⁰⁵, and associate with IFN signaling pathway to maintain body homeostasis³⁶. However, no evidence has shown the relative effect of Regnase-3 deficient mice during disease conditions. At steady state, through TLR3 activation, the expression of Regnase-3 was extremely increased and can be regulated by IFN regulatory factors 3/7 (IRF3/7)³⁶. TLR3 plays an important role in innate immunity through initiating IFN expression, because of its special capacity to identify dsRNA, TLR3 is also paid attention to the treatment of viral diseases such as HIV¹⁰⁶.

Cxcl10 was reported as a pro-inflammatory chemokine and can be induced by IFN- γ ¹⁰⁷, meanwhile it can be secreted by many cells including macrophages¹⁰⁸. IL-10 was found as a key role in mediating organ fibrosis and tissue remodeling during inflammation¹⁰⁹.

All these previous founding implicate that Regnase-3 has the potential to participate in the inflammatory process and host diseases, therefore our data demonstrate that with full knockout Regnase-3, mice at steady state generate inflammation with increased expression of chemokines and cytokines whereas undetectable fibrosis formation and unchanged macrophage number.

5. Macrophage-specific Regnase-3 deficient mice of ANG II Infusion Models

Since there was no fibrosis formation at steady state on Regnase-3 full knockout mice, we try to add some pressure to the hearts of macrophage-specific Regnase-3 ablation mice in order to investigate whether Regnase-3 has a role in degrading extracellular material during ANG II infusion.

We first applied ANG II pump models on LysM-Cre; Regnase-3 flox mice which were specifically deletion of myeloid derived Regnase-3, we found that after 10 days infusion, the fibrosis percentage was increased compared with littermate controls, which means myeloid derived Regnase-3 involved in the process of ANG II induced inflammation and fibrosis formation. However, macrophages have multiple and complex roles in cardiac inflammation and fibrosis formation during chronic inflammatory responses and hypertension. It has been reported that during the first 7 days of ANG II infusion, LysM⁺ macrophages play a key role in pro-inflammatory arterial hypertension with high expressions of M1 macrophage phenotype⁹⁷, however during 2 to 4 weeks, M2 macrophages are predominant in the aorta¹¹⁰. Both M1 and M2-like macrophages participate in the process of inflammation in chronic heart diseases, moreover, cardiac macrophages density increase both results from monocyte recruitment and hematopoietic activation¹¹¹. As known that, LysM-Cre; Regnase-3 flox mice have more effect on the deletion of blood monocytes, during circulation monocytes recruitment to the onset of ANG II induced inflammation in heart, recruited monocytes divided into macrophages and play their important roles in the process of inflammation and fibrosis formation. Since fibrosis is defined by the extracellular matrix accumulation¹¹², without macrophage Regnase-3, the fibrosis formation is increased, which means that myeloid derived Regnase-3 could play a key role in extracellular matrix degradation.

Next, we wanted to figure out what would happen if Regnase-3 deletion in tissue-resident macrophages. We utilized the same mouse model onto the Rank-Cre; Regnase-3 flox mice, interestingly, after ANG II treatment, cardiac fibrosis was decreased compared with littermate controls. This indicated that after deletion Regnase-3 in tissue-resident macrophages, the cardiac fibrosis was attenuated. In order to find out the reason why it's completely the opposite within two mouse lines, flow cytometry and qPCR were then applied to examine the expression of immune cells and related chemokines and cytokines in Rank-Cre; Regnase-3 flox mice heart. Results showed that only Ly6C^{hi} monocytes percentage was increased after treatment, which means compared with control group, blood monocytes were more recruited into heart and played their roles in extracellular matrix degradation. This conclusion is in line with what we found in LysM-Cre; Regnase-3 flox mice after ANG II treatment. However, the reason why blood monocytes were increased recruitment into inflammatory hearts need to be further investigated.

IL-1b and IL-6 are known to involve in the blood pressure modulation⁹⁴, furthermore, IL-6 deficient mice showed attenuated hypertension and reduced cardiac fibrosis in response to ANG II^{113,114}. TGF- β 1 is known to mediate fibrosis formation, during the trans differentiation of fibroblasts to myofibroblasts in heart, it has ability to stimulate mRNA level of IL-6¹¹⁵. It is also shown that during ANG II infusion, IL-6 is primarily produced by cardiac fibroblasts through a macrophages dependent way¹¹⁴. In our experiment of Rank-Cre; Regnase-3 flox mice treated with ANG II, the mRNA expression levels of IL-1b and TGF- β 1 did not change, but the IL-6 was increased, this conclusion is also in line with our previously found that Ly6C^{hi} monocytes were more recruited into heart which then differentiated into pro-inflammatory macrophages. Even through Regnase-3 was knocked out in tissue resident macrophages, the myeloid derived Regnase-3 appears to have a stronger effect in extracellular matrix

degradation.

6. Macrophage-specific Regnase-3 deficient After Ischemia/ Reperfusion

In our study, after MI at day 7, the fibrosis percentage of hearts was increased in the Rank-Cre; Regnase-3 flox mice group compared with littermates, which means without tissue macrophage Regnase-3, degradation of extracellular matrix decreased. However, mRNA levels of inflammatory chemokines and cytokines related to inflammation and fibrosis formation need to be further studied.

In addition, in our experiment, macrophage numbers were also tested both in infarct area and remote area separately by immunohistology of CD68. No statistical difference was observed between groups. Cell counting of blood cells showed that both circulating monocyte number and percentage did not change among other cell types. Together, these data suggest that tissue macrophage Regnase-3 plays its function without changing the numbers of blood monocytes and tissue resident macrophages after myocardial infarction treatment.

7. Outlook

The results presented here indicate that macrophage Regnase-3 has a role in cardiac fibrosis formation. Both myeloid derived and tissue-resident Regnase-3 show this capability under ANG II stress and cardiac injury.

Fibrotic changes in myocardium could lead to a slowdown in electrical conductivity and thus to arrhythmias. An electrophysiological examination, in which cardiac arrhythmias can be provoked and localized by electrodes in the heart, could serve to assess the healing process in these Regnase-3 knockout

mouse models. Moreover, cardiac functions could also change during stress and injury, a cardiac ultrasonography will offer help in diagnosing contraction and diastolic function in the heart. Furthermore, positron emission tomography (PET) can analyze parameters such as the extent of inflammation, the size of infarct area and the pumping function of heart as well. These knowledges will give us a better understanding of Regnase-3 function on hearts.

Further investigation on Regnase-3 of MI models will focus on the gene expression levels of fibrosis related pathways both in LysM-cre and Rank-cre mouse strains. Future experiments will show to what extent we could use the knowledge to develop new therapeutic approaches.

VI. Summary

Within this thesis, the role of macrophage Regnase-3 was investigated both in chronic and acute inflammation in mice heart.

Firstly, under steady state conditions, we checked the cardiac fibrosis formation and macrophage number of Regnase-3-deficient and the knockout-first allele mouse strains, no change was observed compared with their littermate controls. Then, we tried to add some pressure to the hearts. To better understand the different functions of Regnase-3 in myeloid lineage and tissue-resident macrophages, both LysM-Cre; Rgnase-3^{fl/fl} and Rank-Cre; Regnase-3^{fl/fl} mouse strains were applied in our study.

Cardiac chronic inflammation and fibrosis were induced by implanting angiotensin II pumps under the mice's skin, whereas acute inflammation or myocardial infarction was triggered through the ligation of the LAD. After 10 days of angiotensin II infusion, LysM-Cre; Rgnase-3^{fl/fl} mice showed increased cardiac fibrosis formation compared with the control group, however no statistical difference was observed in the adventitia.

On the contrary, the Rank-Cre; Regnase-3^{fl/fl} mice showed decreased cardiac fibrosis compared to littermate controls. However, after 7 days of myocardial infarction, the fibrosis percentage of Rank-Cre; Regnase-3^{fl/fl} mice hearts had a strong trend towards increasing. Both qPCR and flow cytometry were utilized to test the expression of chemokines and cytokines as well as the subtypes of leukocytes in angiotensin II mouse models of Rank-Cre; Regnase-3^{fl/fl} mice.

In summary, it could be shown that macrophage Regnase-3 played an essential role in the process of inflammation and fibrosis formation, but further experiments need to be carried out under intracellular, transcriptome or gene expression levels to develop new therapeutic approaches.

VI. Zusammenfassung

In dieser Arbeit wurde die Rolle des Makrophagen Regnase-3 sowohl bei chronischen als auch bei akuten Entzündungsreaktionen im Herzen von Mäusen untersucht.

Zunächst überprüften wir unter Ruhebedingungen die kardiale Fibrose und die Makrophagenanzahl von Regnase-3-defizienten und die Knockout-First-Allel-Mäusen. Im Vergleich zu den Kontrolltieren wurden keine Veränderung beobachtet.

Dann haben wir versucht, die Herzen in Entzündungsmodellen zu untersuchen. Um die verschiedenen Funktionen von Regnase-3 in myeloiden und gewebsresidenten Makrophagen besser zu verstehen, wurden beide LysM-Cre; Rgnase-3^{fl/fl} und Rank-Cre Tiere in unserer Studie zur Regnase-3 untersucht. Chronische Herzentzündungen und eine Gewebefibrosierung wurden durch Implantation von Angiotensin-II-Pumpen unter die Haut der Mäuse induziert, während akute Entzündungen oder Myokardinfarkte durch die Ligation der LAD Koronararterie ausgelöst wurden. Nach 10 Tagen der Angiotensin II-Infusion wurden LysM-Cre; Rgnase-3^{fl/fl}-Mäuse im Vergleich zur Kontrollgruppe auf eine erhöhte kardiale Fibrose untersucht, jedoch wurde kein statistischer Unterschied in der Adventitia beobachtet.

Im Gegenteil, das Rank-Cre; Regnase-3^{fl/fl}-Mäuse zeigten im Vergleich zu Kontrolltieren eine verminderte kardiale Fibrose. Sieben Tage nach Myokardinfarkt zeigt jedoch die Fibrose in Rank-Cre; Regnase-3^{fl/fl}-Mausherzen einen starken Trend zur Zunahme. Sowohl qPCR als auch Durchflusszytometrie wurden verwendet, um die Expression von Chemokinen und Zytokinen sowie die Subtypen von Leukozyten in Angiotensin-II-Mausmodellen von Rank-Cre zu testen; Regnase-3^{fl/fl}-Mäuse.

Zusammenfassend konnte gezeigt werden, dass die myeloide Regnase-3 eine

wesentliche Rolle im Prozess der Entzündung und Fibrosebildung spielt. Weitere Experimente müssen jedoch unter intrazellulären, Transkriptom- oder Genexpressionsniveaus durchgeführt werden, um neue therapeutische Ansätze zu entwickeln.

VII. Abbreviations

ACE	angiotensin converting enzyme
AGM	aortic-gonadal mesonephros
ANG	angiotensin
AMI	acute myocardial infarction
APC	antigen-presenting cell
AT ₁ R	angiotensin II type-1 receptor
AT ₂ R	angiotensin II type-2 receptor
BBB	blood brain barrier
CABG	coronary artery bypass grafting
CCR2	Chemokine (C-C motif) receptor 2
CCL2	Chemokine (C-C motif) ligand 2
CKMB	creatin kinase myocardial bound
Cxcl10	C-X-C motif chemokine 10
CNS	central nervous system
DAMPs	danger associated molecular patterns
dsRNA	double-stranded ribonucleic acid
ECG	electrocardiography
GFP	green fluorescent protein
GM-CSF	granulocyte-macrophage colony-stimulating factor
HLA	human leucocyte antigen
HMGB1	high mobility group box-1
HSC	hematopoietic stem cell
IFN	interferon
IL	interleukin
IRF	interferon regulatory factor
LAD	left anterior descending artery

LPS	lipopolysaccharide
LV	left ventricular
Ly6C	lymphocyte antigen 6 complex
MAPK	mitogen-activated protein kinase
MCP-1	monocyte chemoattractant protein-1
MCPIP	monocyte chemotactic protein-induced protein
MHC	major histocompatibility complex
MI	myocardial infarction
MMP	matrix metalloproteinase
MPS	mononuclear phagocytosis system
NADPH	nicotinamide adenine dinucleotide phosphate
NF- κ B	nuclear factor κ B
NK	natural killer
NLRs	nucleotide-binding oligomerization-domain protein like receptors
NO	nitric oxide
NSTEMI	non-ST segment elevation myocardial infarction
OPG	osteoprotegerin
PAMPs	pathogen-associated molecular patterns
PDGF	platelet-derived growth factor
PRRs	pattern recognition receptors
PTCA	percutaneous transluminal coronary angioplasty
RAAS	renin-angiotensin-aldosterone system
RAGE	Advanced Glycation End-Products
RANK	receptor of RANKL
RANKL	receptor activator of nuclear factor kappa-B ligand
RNA	ribonucleic acid
ROS	reactive oxygen species
RPM	red pulp macrophage
ssRNA	single-stranded ribonucleic acid
Stat1	Signal transducer and activator of transcription 1

STEMI	ST segment elevation myocardial infarction
TCR	T-cell receptor
TGF- β	transforming growth factor- β
TLR	Toll-like receptor
TNF- α	tumor necrosis factor- α
UTRs	untranslated regions
VCAM-1	vascular cell adhesion molecule-1
VEGF	vascular endothelial growth factor
WGA	wheat germ agglutinin

VIII. Acknowledgement

Three years passed really so fast which at first I thought it would be a long time to go. I can still remember clearly the day I arrived in Munich after more than 10 hours' flight from China, curious and excited. It's truly my honor to be a member of Ludwig Maximilian University of Munich. This experience would be a precious memory of my whole life.

First, I would like to thank my supervisor Prof. Dr. med Christian Schulz for offering me such an opportunity to join and work with this interesting project. I could not get any progress on scientific research without his encouragement, patience, kindness and guidance. When every time we had short meetings talking about my project, he gave me a lot of useful suggestions and ideas, and I think that's why I could learn so much owing to his support and help. Here I sincerely thank him for all the excellent supervision he has provided during these 3 years.

Then, I want to thank my thesis advisory committee, Prof. Dr. med Steffen Massberg and Prof. Dr. med Markus Sperandio. With their being my TAC members, I could start with the project smoothly and improve my research gradually in the lab. Thank them for the valuable comments and insightful opinions which actually give me a lot of confidence to finish my work here.

Third, I would like to thank MMRS, IRTG914, SFB914 for organizing the annual retreats, lectures, seminars, workshops and professional trainings I've ever participated in, they are really of great value. I also thank them for their generous founding. Here I want especially thank Verena Kochan for her help during her busy works, with her patiently and nicely answering all the questions

about my MD structured program, I could eventually get the access to graduate on time.

Furthermore, I would like to thank the China Scholarship Council (CSC) program for offering me with 3 years' financial support, it's really of great help with my daily life abroad without any harassment and struggle. I feel proud of being a member of CSC-LMU cooperation program from the deep of my heart. I will do my best in the rest of my life.

Additionally, I want to thank all my lovely, sweet and adorable colleagues, especially Vanessa Schneider and Denise Messerer, for their kind help with showing me the experiments and the mouse models, Maximilian Fischer, for his helpful suggestions to my project, experiments and thesis, and also Anna Titova, Michael Lorenz, Susanne Sauer, for their work and support to my research. Besides, I want to thank all my Chinese friends I met here in Munich, they encouraged me every time I feel upset, they gave me support every time I need them. We study together, play together, fight together and laugh together, for me, it's really good luck to meet and have them in my colorful life.

Finally, I would like to show my great thanks to my families, my father, my mother and my grandmother. They always understand me and support all the decisions I've made without any hesitation. Meanwhile, I also feel extremely sorry that I could not stay by my grandmother's side during her cancer surgery, however she gives me all the courage that I need to overcome the difficulties on the other side of the world. I couldn't finish my study here without my families. I love them with all my heart.

IX. References

1. Alam R. A brief review of the immune system. *Prim Care*. 1998;25(4):727-738.
2. Delves PJ, Roitt IM. The immune system. First of two parts. *N Engl J Med*. 2000;343(1):37-49.
3. Chaplin DD. 1. Overview of the human immune response. *J Allergy Clin Immunol*. 2006;117(2 Suppl Mini-Primer):S430-435.
4. Mayo L, Quintana FJ, Weiner HL. The innate immune system in demyelinating disease. *Immunol Rev*. 2012;248(1):170-187.
5. Aderem A, Ulevitch RJ. Toll-like receptors in the induction of the innate immune response. *Nature*. 2000;406(6797):782-787.
6. Beutler B, Hoebe K, Du X, Ulevitch RJ. How we detect microbes and respond to them: the Toll-like receptors and their transducers. *J Leukoc Biol*. 2003;74(4):479-485.
7. Nicholson LB. The immune system. *Essays Biochem*. 2016;60(3):275-301.
8. Cavallion JM. The historical milestones in the understanding of leukocyte biology initiated by Elie Metchnikoff. *J Leukoc Biol*. 2011;90(3):413-424.
9. van Furth R, Cohn ZA, Hirsch JG, Humphrey JH, Spector WG, Langevoort HL. The mononuclear phagocyte system: a new classification of macrophages, monocytes, and their precursor cells. *Bull World Health Organ*. 1972;46(6):845-852.
10. van Furth R, Cohn ZA. The origin and kinetics of mononuclear phagocytes. *J Exp Med*. 1968;128(3):415-435.
11. Schulz C, Gomez Perdiguero E, Chorro L, et al. A lineage of myeloid cells independent of Myb and hematopoietic stem cells. *Science*. 2012;336(6077):86-90.
12. Gomez Perdiguero E, Klapproth K, Schulz C, et al. Tissue-resident macrophages originate from yolk-sac-derived erythro-myeloid progenitors. *Nature*. 2015;518(7540):547-551.
13. Hoeffel G, Ginhoux F. Fetal monocytes and the origins of tissue-resident macrophages. *Cell Immunol*. 2018;330:5-15.
14. Sieweke MH, Allen JE. Beyond stem cells: self-renewal of differentiated macrophages. *Science*. 2013;342(6161):1242974.
15. Bertrand JY, Jalil A, Klaine M, Jung S, Cumano A, Godin I. Three pathways to mature macrophages in the early mouse yolk sac. *Blood*. 2005;106(9):3004-3011.
16. Tavian M, Peault B. Embryonic development of the human hematopoietic system. *Int J Dev Biol*. 2005;49(2-3):243-250.
17. Lin WW, Nish SA, Yen B, et al. CD8(+) T Lymphocyte Self-Renewal during Effector Cell Determination. *Cell Rep*. 2016;17(7):1773-1782.
18. Wang B, Zhao L, Fish M, Logan CY, Nusse R. Self-renewing diploid Axin2(+) cells fuel homeostatic renewal of the liver. *Nature*. 2015;524(7564):180-185.
19. Mass E, Ballesteros I, Farlik M, et al. Specification of tissue-resident macrophages during organogenesis. *Science*. 2016;353(6304).
20. Epelman S, Lavine KJ, Beaudin AE, et al. Embryonic and adult-derived resident cardiac macrophages are maintained through distinct mechanisms at steady state and during inflammation. *Immunity*. 2014;40(1):91-104.
21. Molawi K, Wolf Y, Kandalla PK, et al. Progressive replacement of embryo-derived cardiac

- macrophages with age. *J Exp Med*. 2014;211(11):2151-2158.
22. Varol C, Mildner A, Jung S. Macrophages: development and tissue specialization. *Annu Rev Immunol*. 2015;33:643-675.
 23. Heidt T, Courties G, Dutta P, et al. Differential contribution of monocytes to heart macrophages in steady-state and after myocardial infarction. *Circ Res*. 2014;115(2):284-295.
 24. Nahrendorf M, Swirski FK. Monocyte and macrophage heterogeneity in the heart. *Circulation research*. 2013;112(12):1624-1633.
 25. Wynn TA, Chawla A, Pollard JW. Macrophage biology in development, homeostasis and disease. *Nature*. 2013;496(7446):445-455.
 26. Medzhitov R. Origin and physiological roles of inflammation. *Nature*. 2008;454(7203):428-435.
 27. Nowarski R, Gagliani N, Huber S, Flavell RA. Innate immune cells in inflammation and cancer. *Cancer Immunol Res*. 2013;1(2):77-84.
 28. Smigiel KS, Parks WC. Macrophages, Wound Healing, and Fibrosis: Recent Insights. *Current Rheumatology Reports*. 2018;20(4):17.
 29. Gieseck RL, 3rd, Wilson MS, Wynn TA. Type 2 immunity in tissue repair and fibrosis. *Nat Rev Immunol*. 2018;18(1):62-76.
 30. Liang J, Wang J, Azfer A, et al. A novel CCCH-zinc finger protein family regulates proinflammatory activation of macrophages. *J Biol Chem*. 2008;283(10):6337-6346.
 31. Matsushita K, Takeuchi O, Standley DM, et al. Zc3h12a is an RNase essential for controlling immune responses by regulating mRNA decay. *Nature*. 2009;458(7242):1185-1190.
 32. Kawai T, Akira S. The role of pattern-recognition receptors in innate immunity: update on Toll-like receptors. *Nature Immunology*. 2010;11(5):373-384.
 33. Mino T, Takeuchi O. Regnase-1 and Roquin regulate inflammatory mRNAs. *Oncotarget*. 2015;6(20):17869-17870.
 34. de Bruin RG, Rabelink TJ, van Zonneveld AJ, van der Veer EP. Emerging roles for RNA-binding proteins as effectors and regulators of cardiovascular disease. *Eur Heart J*. 2017;38(18):1380-1388.
 35. Blech-Hermoni Y, Ladd AN. RNA binding proteins in the regulation of heart development. *The international journal of biochemistry & cell biology*. 2013;45(11):2467-2478.
 36. von Gamm M, Schaub A, Jones AN, et al. Immune homeostasis and regulation of the interferon pathway require myeloid-derived Regnase-3. *J Exp Med*. 2019;216(7):1700-1723.
 37. Zhou SS, Jin JP, Wang JQ, et al. miRNAs in cardiovascular diseases: potential biomarkers, therapeutic targets and challenges. *Acta Pharmacol Sin*. 2018;39(7):1073-1084.
 38. Drazner MH. The progression of hypertensive heart disease. *Circulation*. 2011;123(3):327-334.
 39. Snijder PM, Frenay AR, de Boer RA, et al. Exogenous administration of thiosulfate, a donor of hydrogen sulfide, attenuates angiotensin II-induced hypertensive heart disease in rats. *Br J Pharmacol*. 2015;172(6):1494-1504.
 40. Letavernier E, Perez J, Bellocq A, et al. Targeting the calpain/calpastatin system as a new strategy to prevent cardiovascular remodeling in angiotensin II-induced hypertension. *Circ Res*. 2008;102(6):720-728.

41. Navar LG, Nishiyama A. Intrarenal formation of angiotensin II. *Contrib Nephrol.* 2001(135):1-15.
42. Azushima K, Morisawa N, Tamura K, Nishiyama A. Recent Research Advances in Renin-Angiotensin-Aldosterone System Receptors. *Curr Hypertens Rep.* 2020;22(3):22.
43. Patel S, Rauf A, Khan H, Abu-Izneid T. Renin-angiotensin-aldosterone (RAAS): The ubiquitous system for homeostasis and pathologies. *Biomed Pharmacother.* 2017;94:317-325.
44. Zeng S-Y, Luo J-F, Quan H-Y, et al. Protein Arginine Methyltransferase 2 Inhibits Angiotensin II-Induced Proliferation and Inflammation in Vascular Smooth Muscle Cells. *Biomed Res Int.* 2018;2018:1547452-1547452.
45. Chen Y, Arrigo A-P, Currie RW. Heat shock treatment suppresses angiotensin II-induced activation of NF- κ B pathway and heart inflammation: a role for IKK depletion by heat shock? *American Journal of Physiology-Heart and Circulatory Physiology.* 2004;287(3):H1104-H1114.
46. Agita A, Alsagaff MT. Inflammation, Immunity, and Hypertension. *Acta Med Indones.* 2017;49(2):158-165.
47. Williams B, Baker AQ, Gallacher B, Lodwick D. Angiotensin II increases vascular permeability factor gene expression by human vascular smooth muscle cells. *Hypertension.* 1995;25(5):913-917.
48. Zhan Y, Brown C, Maynard E, et al. Ets-1 is a critical regulator of Ang II-mediated vascular inflammation and remodeling. *J Clin Invest.* 2005;115(9):2508-2516.
49. Swirski FK, Nahrendorf M, Etzrodt M, et al. Identification of splenic reservoir monocytes and their deployment to inflammatory sites. *Science.* 2009;325(5940):612-616.
50. Sun Y, Ramires FJ, Zhou G, Ganjam VK, Weber KT. Fibrous tissue and angiotensin II. *J Mol Cell Cardiol.* 1997;29(8):2001-2012.
51. Wynn TA. Cellular and molecular mechanisms of fibrosis. *J Pathol.* 2008;214(2):199-210.
52. Wynn TA. Common and unique mechanisms regulate fibrosis in various fibroproliferative diseases. *J Clin Invest.* 2007;117(3):524-529.
53. Bacmeister L, Schwarzl M, Warnke S, et al. Inflammation and fibrosis in murine models of heart failure. *Basic Res Cardiol.* 2019;114(3):19.
54. Kyselovic J, Leddy JJ. Cardiac Fibrosis: The Beneficial Effects of Exercise in Cardiac Fibrosis. *Adv Exp Med Biol.* 2017;999:257-268.
55. Kuwahara F, Kai H, Tokuda K, et al. Transforming growth factor-beta function blocking prevents myocardial fibrosis and diastolic dysfunction in pressure-overloaded rats. *Circulation.* 2002;106(1):130-135.
56. Kelly DJ, Cox AJ, Gow RM, Zhang Y, Kemp BE, Gilbert RE. Platelet-derived growth factor receptor transactivation mediates the trophic effects of angiotensin II in vivo. *Hypertension.* 2004;44(2):195-202.
57. Crowley SD, Gurley SB, Herrera MJ, et al. Angiotensin II causes hypertension and cardiac hypertrophy through its receptors in the kidney. *Proc Natl Acad Sci U S A.* 2006;103(47):17985-17990.
58. Bush E, Maeda N, Kuziel WA, et al. CC chemokine receptor 2 is required for macrophage infiltration and vascular hypertrophy in angiotensin II-induced hypertension. *Hypertension.* 2000;36(3):360-363.

59. Stawski L, Haines P, Fine A, Rudnicka L, Trojanowska M. MMP-12 deficiency attenuates angiotensin II-induced vascular injury, M2 macrophage accumulation, and skin and heart fibrosis. *PLoS One*. 2014;9(10):e109763.
60. Prabhu SD, Frangogiannis NG. The Biological Basis for Cardiac Repair After Myocardial Infarction: From Inflammation to Fibrosis. *Circ Res*. 2016;119(1):91-112.
61. Spath NB, Mills NL, Cruden NL. Novel cardioprotective and regenerative therapies in acute myocardial infarction: a review of recent and ongoing clinical trials. *Future Cardiol*. 2016;12(6):655-672.
62. Francis Stuart SD, De Jesus NM, Lindsey ML, Ripplinger CM. The crossroads of inflammation, fibrosis, and arrhythmia following myocardial infarction. *Journal of molecular and cellular cardiology*. 2016;91:114-122.
63. Eltzschig HK, Eckle T. Ischemia and reperfusion--from mechanism to translation. *Nat Med*. 2011;17(11):1391-1401.
64. Lambert JM, Lopez EF, Lindsey ML. Macrophage roles following myocardial infarction. *Int J Cardiol*. 2008;130(2):147-158.
65. de Haan JJ, Smeets MB, Pasterkamp G, Arslan F. Danger signals in the initiation of the inflammatory response after myocardial infarction. *Mediators Inflamm*. 2013;2013:206039.
66. Cirillo P, Giallauria F, Pacileo M, et al. Increased high mobility group box-1 protein levels are associated with impaired cardiopulmonary and echocardiographic findings after acute myocardial infarction. *J Card Fail*. 2009;15(4):362-367.
67. Newton K, Dixit VM. Signaling in innate immunity and inflammation. *Cold Spring Harb Perspect Biol*. 2012;4(3).
68. Mann DL. The emerging role of innate immunity in the heart and vascular system: for whom the cell tolls. *Circ Res*. 2011;108(9):1133-1145.
69. Lu C, Ren D, Wang X, et al. Toll-like receptor 3 plays a role in myocardial infarction and ischemia/reperfusion injury. *Biochim Biophys Acta*. 2014;1842(1):22-31.
70. Arslan F, Smeets MB, O'Neill LA, et al. Myocardial ischemia/reperfusion injury is mediated by leukocytic toll-like receptor-2 and reduced by systemic administration of a novel anti-toll-like receptor-2 antibody. *Circulation*. 2010;121(1):80-90.
71. Oyama J, Blais C, Jr., Liu X, et al. Reduced myocardial ischemia-reperfusion injury in toll-like receptor 4-deficient mice. *Circulation*. 2004;109(6):784-789.
72. Maekawa N, Wada H, Kanda T, et al. Improved myocardial ischemia/reperfusion injury in mice lacking tumor necrosis factor- α . *J Am Coll Cardiol*. 2002;39(7):1229-1235.
73. Fuchs M, Hilfiker A, Kaminski K, et al. Role of interleukin-6 for LV remodeling and survival after experimental myocardial infarction. *FASEB J*. 2003;17(14):2118-2120.
74. Nahrendorf M, Pittet MJ, Swirski FK. Monocytes: protagonists of infarct inflammation and repair after myocardial infarction. *Circulation*. 2010;121(22):2437-2445.
75. Nahrendorf M, Swirski FK, Aikawa E, et al. The healing myocardium sequentially mobilizes two monocyte subsets with divergent and complementary functions. *J Exp Med*. 2007;204(12):3037-3047.
76. Ma Y, Mouton AJ, Lindsey ML. Cardiac macrophage biology in the steady-state heart, the aging heart, and following myocardial infarction. *Transl Res*. 2018;191:15-28.
77. Leuschner F, Rauch PJ, Ueno T, et al. Rapid monocyte kinetics in acute myocardial infarction are sustained by extramedullary monocytopoiesis. *J Exp Med*. 2012;209(1):123-

- 137.
78. Tsujioka H, Imanishi T, Ikejima H, et al. Impact of heterogeneity of human peripheral blood monocyte subsets on myocardial salvage in patients with primary acute myocardial infarction. *J Am Coll Cardiol*. 2009;54(2):130-138.
 79. Frantz S, Nahrendorf M. Cardiac macrophages and their role in ischaemic heart disease. *Cardiovasc Res*. 2014;102(2):240-248.
 80. Lee WW, Marinelli B, van der Laan AM, et al. PET/MRI of inflammation in myocardial infarction. *Journal of the American College of Cardiology*. 2012;59(2):153-163.
 81. Ismahil MA, Hamid T, Bansal SS, Patel B, Kingery JR, Prabhu SD. Remodeling of the mononuclear phagocyte network underlies chronic inflammation and disease progression in heart failure: critical importance of the cardiosplenic axis. *Circulation research*. 2014;114(2):266-282.
 82. Lavine KJ, Epelman S, Uchida K, et al. Distinct macrophage lineages contribute to disparate patterns of cardiac recovery and remodeling in the neonatal and adult heart. *Proceedings of the National Academy of Sciences of the United States of America*. 2014;111(45):16029-16034.
 83. Aurora AB, Porrello ER, Tan W, et al. Macrophages are required for neonatal heart regeneration. *J Clin Invest*. 2014;124(3):1382-1392.
 84. Yap J, Cabrera-Fuentes HA, Irei J, Hausenloy DJ, Boisvert WA. Role of Macrophages in Cardioprotection. *Int J Mol Sci*. 2019;20(10):2474.
 85. Jung K, Kim P, Leuschner F, et al. Endoscopic time-lapse imaging of immune cells in infarcted mouse hearts. *Circulation research*. 2013;112(6):891-899.
 86. Dutta P, Nahrendorf M. Monocytes in myocardial infarction. *Arterioscler Thromb Vasc Biol*. 2015;35(5):1066-1070.
 87. Yan X, Anzai A, Katsumata Y, et al. Temporal dynamics of cardiac immune cell accumulation following acute myocardial infarction. *J Mol Cell Cardiol*. 2013;62:24-35.
 88. ter Horst EN, Hakimzadeh N, van der Laan AM, Krijnen PAJ, Niessen HWM, Piek JJ. Modulators of Macrophage Polarization Influence Healing of the Infarcted Myocardium. *Int J Mol Sci*. 2015;16(12):29583-29591.
 89. Troidl C, Möllmann H, Nef H, et al. Classically and alternatively activated macrophages contribute to tissue remodelling after myocardial infarction. *J Cell Mol Med*. 2009;13(9B):3485-3496.
 90. Piek A, de Boer RA, Silljé HHW. The fibrosis-cell death axis in heart failure. *Heart Fail Rev*. 2016;21(2):199-211.
 91. Frangogiannis NG. Cardiac fibrosis: Cell biological mechanisms, molecular pathways and therapeutic opportunities. *Mol Aspects Med*. 2019;65:70-99.
 92. Jacome-Galarza CE, Percin GI, Muller JT, et al. Developmental origin, functional maintenance and genetic rescue of osteoclasts. *Nature*. 2019;568(7753):541-545.
 93. Bustin SA. Quantification of mRNA using real-time reverse transcription PCR (RT-PCR): trends and problems. *J Mol Endocrinol*. 2002;29(1):23-39.
 94. Crowley SD, Song Y-S, Sprung G, et al. A role for angiotensin II type 1 receptors on bone marrow-derived cells in the pathogenesis of angiotensin II-dependent hypertension. *Hypertension (Dallas, Tex : 1979)*. 2010;55(1):99-108.
 95. Wang J, He W, Guo L, et al. The ACE2-Ang (1-7)-Mas receptor axis attenuates cardiac

- remodeling and fibrosis in post-myocardial infarction. *Mol Med Rep.* 2017;16(2):1973-1981.
96. Cross M, Renkawitz R. Repetitive sequence involvement in the duplication and divergence of mouse lysozyme genes. *EMBO J.* 1990;9(4):1283-1288.
97. Wenzel P, Knorr M, Kossmann S, et al. Lysozyme M-positive monocytes mediate angiotensin II-induced arterial hypertension and vascular dysfunction. *Circulation.* 2011;124(12):1370-1381.
98. Abram CL, Roberge GL, Hu Y, Lowell CA. Comparative analysis of the efficiency and specificity of myeloid-Cre deleting strains using ROSA-EYFP reporter mice. *J Immunol Methods.* 2014;408:89-100.
99. Weber KT, Swamynathan SK, Guntaka RV, Sun Y. Angiotensin II and extracellular matrix homeostasis. *Int J Biochem Cell Biol.* 1999;31(3-4):395-403.
100. Antoniak S, Cardenas JC, Buczek LJ, Church FC, Mackman N, Pawlinski R. Protease-Activated Receptor 1 Contributes to Angiotensin II-Induced Cardiovascular Remodeling and Inflammation. *Cardiology.* 2017;136(4):258-268.
101. Luo J, Chen X, Luo C, et al. Hydrochlorothiazide modulates ischemic heart failure-induced cardiac remodeling via inhibiting angiotensin II type 1 receptor pathway in rats. *Cardiovasc Ther.* 2017;35(2).
102. Emde B, Heinen A, Gödecke A, Bottermann K. Wheat germ agglutinin staining as a suitable method for detection and quantification of fibrosis in cardiac tissue after myocardial infarction. *Eur J Histochem.* 2014;58(4):2448-2448.
103. Gerstberger S, Hafner M, Tuschl T. A census of human RNA-binding proteins. *Nat Rev Genet.* 2014;15(12):829-845.
104. Mino T, Murakawa Y, Fukao A, et al. Regnase-1 and Roquin Regulate a Common Element in Inflammatory mRNAs by Spatiotemporally Distinct Mechanisms. *Cell.* 2015;161(5):1058-1073.
105. Tsoi LC, Spain SL, Knight J, et al. Identification of 15 new psoriasis susceptibility loci highlights the role of innate immunity. *Nat Genet.* 2012;44(12):1341-1348.
106. Zhou Y, Guo M, Wang X, et al. TLR3 activation efficiency by high or low molecular mass poly I:C. *Innate Immun.* 2013;19(2):184-192.
107. Schnabel CL, Babasyan S, Freer H, Wagner B. CXCL10 production in equine monocytes is stimulated by interferon-gamma. *Vet Immunol Immunopathol.* 2019;207:25-30.
108. Lee J-H, Kim B, Jin WJ, Kim H-H, Ha H, Lee ZH. Pathogenic roles of CXCL10 signaling through CXCR3 and TLR4 in macrophages and T cells: relevance for arthritis. *Arthritis Res Ther.* 2017;19(1):163-163.
109. Sziksz E, Pap D, Lippai R, et al. Fibrosis Related Inflammatory Mediators: Role of the IL-10 Cytokine Family. *Mediators of inflammation.* 2015;2015:764641-764641.
110. Moore JP, Vinh A, Tuck KL, et al. M2 macrophage accumulation in the aortic wall during angiotensin II infusion in mice is associated with fibrosis, elastin loss, and elevated blood pressure. *Am J Physiol Heart Circ Physiol.* 2015;309(5):H906-917.
111. Hulsmans M, Sager HB, Roh JD, et al. Cardiac macrophages promote diastolic dysfunction. *J Exp Med.* 2018;215(2):423-440.
112. Wynn TA, Ramalingam TR. Mechanisms of fibrosis: therapeutic translation for fibrotic disease. *Nat Med.* 2012;18(7):1028-1040.

113. Lee DL, Sturgis LC, Labazi H, et al. Angiotensin II hypertension is attenuated in interleukin-6 knockout mice. *Am J Physiol Heart Circ Physiol.* 2006;290(3):H935-940.
114. Ma F, Li Y, Jia L, et al. Macrophage-stimulated cardiac fibroblast production of IL-6 is essential for TGF β /Smad activation and cardiac fibrosis induced by angiotensin II. *PLoS One.* 2012;7(5):e35144.
115. Seong GJ, Hong S, Jung SA, et al. TGF-beta-induced interleukin-6 participates in transdifferentiation of human Tenon's fibroblasts to myofibroblasts. *Mol Vis.* 2009;15:2123-2128.